Geochemical bio-signatures in Martian analogue basaltic environments using laboratory experiments and thermochemical modelling

frontiers | Frontiers in Astronomy and Space Sciences

TYPE Original Research
PUBLISHED 17 November 2022
DOI 10.3389/fspas.2022.1062007

OPEN ACCESS

EDITED BY
Barbara Cavalazzi,
University of Bologna, Italy

REVIEWED BY
Eva Mateo-Marti,
Center for Astrobiology (CSIC), Spain
Ricardo Amils,
Autonomous University of Madrid, Spain

*CORRESPONDENCE
Simone Cogliati,
s.cogliati86@gmail.com

SPECIALTY SECTION
This article was submitted to Astrobiology,
a section of the journal
Frontiers in Astronomy and Space Sciences

RECEIVED 05 October 2022
ACCEPTED 04 November 2022
PUBLISHED 17 November 2022

CITATION
Cogliati S, Wolsey E, Ramkissoon NK, Schwenzer SP, Pearson VK and Olsson-Francis K (2022), Geochemical bio-signatures in Martian analogue basaltic environments using laboratory experiments and thermochemical modelling.
Front. Astron. Space Sci. 9:1062007.
doi: 10.3389/fspas.2022.1062007

Geochemical bio-signatures in Martian analogue basaltic environments using laboratory experiments and thermochemical modelling

Simone Cogliati*, Elliot Wolsey, Nisha K. Ramkissoon, Susanne P. Schwenzer, Victoria K. Pearson and Karen Olsson-Francis

AstrobiologyOU, Faculty of Science and Technology, Engineering and Mathematics, The Open University, Milton Keynes, United Kingdom

The identification of geochemical bio-signatures is important for assessing whether life existed on early Mars. In this paper, experimental microbiology and thermochemical modelling were combined to identify potential inorganic bio-signatures for life detection on early Mars. An analogue mixed microbial community from an analogue terrestrial fluvio-lacustrine environment similar to an ancient lacustrine system at Gale Crater was used to study microbial dissolution of a basalt regolith simulant and the formation of bio-signatures over a short time frame (1˚month) at 14˚C, 2 bar. Microbial growth influenced element dissolution (Mg, Fe, Mn, Ca and K) and the formation of morphologies and Fe-Si amorphous layers on mineral surfaces. Thermochemical models were performed at 14˚C, 2 bar; the results were compared with experimental data to predict bio-signatures that would occur over geological timescales. The pH was varied to simulate abiotic and biotic experimental conditions. Model results suggest that, at water to rock ratios of 100 to 38, a less complex secondary mineral assemblage forms during biotic dissolution compared to abiotic weathering. Carbonates, quartz, pyrite and hydroxyapatite form under biotic conditions, whereas in the abiotic system magnetite and phyllosilicates would also precipitate. These results could be used to distinguish between abiotic and biotic basalt weathering processes, aiding the interpretation of data from Mars exploration missions.

KEYWORDS

Mars, Mars bio-signatures, terrestrial analogue, thermochemical modelling, microbiology

1 Introduction

Finding evidence of past or present life on Mars is one of the key objectives of the most recent and future space exploration missions (NASA's Mars Science Laboratory, NASA's Mars 2020, and ESA's ExoMars—Grotzinger et al., 2012; Vago et al., 2017; Ehrenfried, 2022). Since water is essential for life as we know it, most of the efforts are focused on the investigation of potentially habitable extraterrestrial aqueous environments where water may have existed, or still exists. Geological, geochemical and geomorphological evidence collected by orbiting spacecraft, landers and rovers (e.g., Mars Odyssey, Curiosity, Opportunity, Mars Express) suggest that early Mars had a denser atmosphere, warmer surface temperatures, and more clement and less oxidising environmental conditions than today (e.g. Carr and Head, 2010; Mangold et al., 2012) that may have been conducive to life (Molina-Cuberos et al., 2001; Bibring et al., 2005; Tian et al., 2009). Among other places, impact-generated hydrothermal systems (Schwenzer and Kring, 2009; Marzo et al., 2010; Mangold et al., 2012; Schwenzer et al., 2012; Osinski et al., 2013; Arvidson et al., 2014; Fox et al., 2016; Turner et al., 2016) and fluvio-lacustrine systems (e.g., Gale and Jezero Craters—Grotzinger et al., 2014; Grotzinger et al., 2015; Rampe et al., 2017; Mangold et al., 2021; Tu et al., 2021) identified on Mars may have been habitable (Malin and Edgett, 2003; Abramov and Kring, 2005; Irwin et al., 2005; Mangold et al., 2012; Williams et al., 2013; Grotzinger et al., 2014; Fassett and Head, 2015) in the Noachian—early Hesperian (4.1–3.0 Ga, Grotzinger et al., 2014). It has been suggested that Gale Crater's aqueous environment had a circumneutral pH, temperatures suitable for low salinity water bodies (e.g., lake, rivers) that were stable over geological timescales, a varied chemical history and sedimentological features that can be associated with complex aqueous processes and potentially diverse redox conditions that may have been used as an energy source for life (Grotzinger et al., 2014; Bridges et al., 2015; Hurowitz et al., 2017; Edgar et al., 2020; Fraeman et al., 2020; Rampe et al., 2020; Ramkissoon et al., 2021; Rapin et al., 2021).

Since rocks of basaltic composition dominate the Martian surface (Nyquist et al., 2001; Christensen et al., 2005; Filiberto, 2008; Treiman and Filiberto, 2015; Morris et al., 2016; Mangold et al., 2017), weathering processes and/or brine evaporation has evolved clay minerals, carbonates, sulfates and other alteration minerals (Poulet et al., 2005; Poulet et al., 2007; Ehlmann et al., 2008; Mustard et al., 2008; Ehlmann et al., 2009; Bridges et al., 2015; Stern et al., 2015; Bultel et al., 2019; Horgan et al., 2020). The presence of such secondary minerals, for example at Gale and Jezero Craters, indicates a variety of alteration conditions and water-rock reactions that may have controlled the local chemical conditions (e.g., chemistry of the fluids, redox state of elements, release of elements into the fluids) and, thus, the availability of bio-essential elements. Understanding the formation of secondary minerals is therefore critical to determining the potential habitability of aqueous environments (Schulte et al., 2006; Hand et al., 2007; Bridges and Schwenzer, 2012).

In terrestrial aqueous systems, the chemistry of alteration products and the reactions occurring in each system are influenced by the local environmental conditions, parent rock mineralogy and permeability, water-to-rock ratios, duration of alteration, and the presence of microbes (Boston et al., 2001; Wu et al., 2007; Schwenzer and Kring, 2009; Ehlmann et al., 2013; Bridges et al., 2015; Carter et al., 2015; Olsson-Francis et al., 2015; Zolotov and Mironenko, 2016). Laboratory experiments, among other insights, have shown that microbes can enhance basalt weathering rates sourcing bio-essential elements from olivine, pyroxene and plagioclase (e.g. Vandevivere et al., 1994; Barker et al., 1998; Rogers et al., 1998; Kalinowski et al., 2000; Liermann et al., 2000; Bennet et al., 2001; Welch et al., 2002; Wu et al., 2007; Uroz et al., 2009; Olsson-Francis et al., 2015; Olsson-Francis et al., 2017), whereby microbes use multiple mechanisms to extract bio-essential elements from basaltic rocks including the production of excess protons, low molecular weight organic acids, siderophores (highly specific Fe^{3+} ligands) and extracellular polysaccharides and enzymes (Welch and Ullman, 1993; Vandevivere et al., 1994; Barker et al., 1998; Bennet et al., 2001; Wu et al., 2007; Olsson-Francis et al., 2015). Some of these processes can leave specific chemical and mineralogical signatures in the rocks that indicate the former presence of life.

Bio-signatures are formed by microbial activity (e.g., Vandevivere et al., 1994; Banfield et al., 2001; Westall et al., 2015; Price et al., 2018; Tan et al., 2018) and can be divided in two main categories: 1) organic bio-signatures, which are biomolecules produced by organisms as part of their metabolic and reproductive machinery (Summons et al., 2011; Röling et al., 2015; Westall et al., 2015; Hays et al., 2017; Vago et al., 2017); and 2) inorganic bio-signatures, which include morphological fossils, sedimentary structures, isotope fractionation, and mineral alterations that are the result of microbial activity (Banfield et al., 2001; Cady et al., 2003; Westall et al., 2015; Vago et al., 2017; McMahon et al., 2018). Such bio-signatures can be preserved within the geological record and used as evidence of the presence of life in terrestrial and extraterrestrial environments, including early Martian aqueous systems. Owing to the detrimental effect of the conditions at the present-day surface of Mars, which can degrade organic molecules (Ten Kate et al., 2005; Dartnell, 2011; Hays et al., 2017; Vago et al., 2017), inorganic bio-signatures, such as secondary alteration minerals, may be more appropriate for assessing whether life existed on early Mars. For example, biotically produced secondary minerals may be preserved in Martian rocks and be detectable through *in-situ* measurements by on-going and up-coming rover missions (Vago et al., 2017).

To identify and use, unambiguously, specific secondary mineral assemblages as bio-signatures for life detection, it is fundamental to have a comprehensive comparison between biotic and abiotic weathering processes. Investigating analogue environments is one way of informing our understanding of potential bio-signatures. Unfortunately, the heterogeneity of the natural environment, the lack of control over changes during even a short sampling period, and the difficulty of finding relevant abiotic controls, make such work challenging. Moreover, although basalt weathering and secondary alteration mineral formation have been widely investigated in the field and in laboratory experiments under abiotic (Gislason and Eugster, 1987; Oelkers and Gislason, 2001; Wolff-Boenisch et al., 2006) and biotic conditions (Wu et al., 2007; Olsson-Francis et al., 2010; Olsson-Francis et al., 2012; Olsson-Francis et al., 2015; Olsson-Francis et al., 2016; Olsson-Francis et al., 2017; Price et al., 2018; Olsson-Francis et al., 2020) these studies have been only over short timeframes (months—years). This makes it difficult, if not impossible, to predict what would happen over years or even over geological time scales when the rock is fully dissolved or more likely, subject to the effects of incongruent dissolution. In these circumstances, the formation of amorphous and leached layers, and secondary mineral precipitation, may occur, influencing the availability of cations for use in biological metabolism and, thus, the formation of bio-signatures (e.g. Welch and Ullman, 1993; Benzerara et al., 2004; Benzerara et al., 2005).

In order to overcome this problem, thermochemical modelling can be used to study, theoretically, alteration processes that can occur over geological timescales. Owing to its capability to predict secondary mineral assemblages and variations in fluid chemistries by assessing reaction pathways during water-rock interactions, thermochemical modelling has been widely applied to study alteration processes that happened, or may have happened, in terrestrial and Martian aqueous environments (Griffith and Shock, 1997; Kühn, 2004; Zolotov and Mironenko, 2007; Marion et al., 2008; Bridges and Schwenzer, 2012; Catalano, 2013; Filiberto and Schwenzer, 2013; Schwenzer and Kring, 2013; Bridges et al., 2015; Melwani Daswani et al., 2016; Zolotov and Mironenko, 2016; Ramkissoon et al., 2021). Only recently, Olsson-Francis et al. (2017) used thermochemical modelling in conjunction with laboratory-based experiments to investigate and compare the alteration minerals that may form during microbial basalt weathering over a range of different timescales. The study suggested that an aerobic chemoorganoheterotrophic bacterium (*Burkholderia* sp. strain B_33), during long-term weathering of a naturally occurring altered basalt, would produce a less chemically and mineralogically diverse secondary mineral assemblage consisting of Fe-hydroxide and kaolinite, than under abiotic conditions, where chlorite would also be formed (Olsson-Francis et al., 2017). That study also demonstrated the utility of combining laboratory experiments and thermochemical modelling to identify secondary minerals that could be used to distinguish, unambiguously, weathering processes that may have occurred on early Mars (Olsson-Francis et al., 2017).

In this paper, we investigate the impact of microbial activity on a simulated Rocknest environment and the formation of inorganic bio-signatures using a combination of laboratory-based experiments and thermochemical modelling. The Rocknest environment was simulated by preparing a Martian regolith simulant with a composition similar to that of the Rocknest basalts (global Martian basaltic soils, Blake et al., 2013; Schmidt et al., 2014) and combining this with a minimal medium. A buffer was added to the medium to compensate for the reactions that would occur between the basalt and a CO_2 rich headspace, with the intent to create a stable environment with circumneutral pH (Bridges and Schwenzer, 2012) similar to ancient Martian aqueous systems (Grotzinger et al., 2014; Vaniman et al., 2014). To study the fluid chemistry variations and secondary minerals formed under biotic conditions we use a terrestrial analogue mixed anaerobic community consisting of chemoorganotrophs and chemolithotrophs. The analogue microbial community was isolated from a Mars analogue environment, the anoxic intertidal zone of the River Dee (United Kingdom), and had previously been deemed a plausible analogue to study habitability of ancient lacustrine systems on early Mars (e.g. Gale Crater) using laboratory-based simulation experiments (Curtis-Harper et al., 2018).

Experimental and model results were compared in order to identify chemical and mineralogical signatures that are uniquely produced by microbial weathering and may be used as inorganic bio-signatures for life detection on Mars. Instrumentation onboard current Martian rovers could provide mineralogical and geochemical data that would assist in the identification of potential bio-signatures, e.g., the CheMin (XRD) instrument and the Laser Induced Breakdown Spectroscopy (LIBS, ChemCam) and the Alpha Particle X-Ray Spectrometer (APXS) instrument on board of the Mars Science Laboratory Rover Curiosity (Grotzinger et al., 2012) and the most recent SuperCam (a LIBS instrument) and Raman instruments on board of the Perseverance rover (Williford et al., 2008).

2 Methods

2.1 Preparation and characterization of the mars regolith simulant

For this study, a regolith simulant was prepared that was compositionally similar to basaltic float rocks analysed by

TABLE 1 Major element composition of the basalt, aegirine and regolith simulant in comparison to Rocknest composition.

Oxide (wt%)	Basalt	Aegirine	Regolith analogue	Rocknest*
SiO_2	44.7	52.35	47.48	45.98
$Fe_2O_{3(T)}$	11.73	29.21	18.09	18.38
MnO	0.21	0.66	0.38	0.45
MgO	4.66	0.07	2.99	5.33
Na_2O	4.02	12.21	7	4.02
K_2O	2.37	-	1.51	1.86
P_2O_5	0.93	0.01	0.6	1.08
Cl	-	-	-	0.88
SO3	-	0.03	0.01	-
TiO2	-	0.9	0.33	-
Al_2O_3	-	0.19	0.07	-
CaO	-	1.52	0.55	-
NiO	-	0.01	0	-

*Composition from Schmidt et al., 2014.

Curiosity at Rocknest, Gale Crater (Schmidt et al., 2014) (Table 1). The simulant consisted of basalt from Le Cheix Puy de Dome (France) (Table 1), which was selected to represent a typical unweathered basalt, whereby any macroscopically visible weathering was separated out of the sample during the sample preparation. The basalt was supplemented with aegirine, an iron rich pyroxene (FeO 29.21 wt%, Table 1) from Mount Malosa (Malawi). This was to ensure that the simulant contained an equivalent iron content to an average Martian basalt, which is higher than terrestrial basalts (Longhi et al., 1992), and to correct for Fe speciation. This is important when exploring Martian habitability since the Fe^{2+}/Fe^{3+} ratio is crucial for microbial metabolism (Nixon et al., 2013; Ramkissoon et al., 2021). Both the basalt and the aegirine were purchased from Richard Tayler Minerals (United Kingdom).

The major element composition of the aegirine (Table 1) was obtained from polished thin sections using a CAMECA SX100 Electron Microprobe (EMPA) operated with a spot size of 10 mm, accelerating voltage of 20 kV and a beam current of 20 nA. Analysis of the basalt's major element composition (Table 1) was carried out on powdered samples using an ARL 8,420 + dual goniometer wavelength-dispersive X-ray Fluorescence (XRF) spectrometer.

To produce the regolith simulant, the basalt and aegirine were separately crushed using a Tema swing mill, for 8 min. The crushed materials were sieved to a fraction size of between 100 µm and 250 µm, the fine particles were removed by ultrasonication in MilliQ water (Olsson-Francis et al., 2010; Olsson-Francis et al., 2017), and the products were dried for 24 h, at 80 C and at 1 bar. The 100–250 µm size fraction was selected to include materials that have a grain size comparable to dust-size particles of the Martian regolith observed by Curiosity's Mars Hand Lens Imager instrument in sedimentary deposits at various locations at Gale crater (Minitti et al., 2013; Weitz et al., 2018). Moreover, the selection of a such small grain size was intended to speed up the formation of secondary minerals mitigating for the short duration of the dissolution experiments. The aegirine was mixed to the basalt in a 1.75:1 ratio to achieve an overall iron-rich composition similar to that of Rocknest basalt (Schmidt et al., 2014), which has 6.65 wt% more $Fe_2O_{3(Tot)}$ than the Le Cheix Puy de Dome basalt (Table 1).

TABLE 2 Relative abundance of the bacterial families from the anoxic intertidal zone of the River Dee estuary. Data obtained from MiSeq DNA gene sequences. A detailed description and characterization of the microbial community and how it was sampled is given in Curtis-Harper et al. (2018).

Bacterial families	Proportion %
Hyphomicrobiaceae	28
Flavobacteriaceae	23
Alteromonadaceae	16
Rhodobiaceae	10
Rhodobacteraceae	6
Acidimicrobiales	6
Caldilineaceae	3
Peptostreptococcaceae	1
Flammeovirgaceae	1
Nitrospiraceae	1
Desulfobacteraceae	1
Granulosicoccaceae	1
Rhodospirillaceae	1
Others	2

2.2 Microbial community

A microbial community from the sub-surface intertidal anoxic zone of the River Dee, United Kingdom (53°21′15.40 N, 3°10′24.95 W) was used for the biotic experiments. This mixed community was selected because it contains chemolithoautotrophic and chemoorganoheterotrophic microbes that are analogues for potential microbial life that may have existed in the fluvio-lacustrine environment at Gale Crater (Amils et al., 2007; Grotzinger et al., 2014; Curtis-Harper et al., 2018). The sample was collected as part of a previous study (Curtis-Harper et al., 2018). MiSeq sequencing demonstrated that the bacterial community was dominated by the families Hyphomicrobiaceae (28%), Flavobacteriaceae (23%), Alteromonadaceae (16%), whilst over 90% of the archaeal community was dominated by *Thaumarchaeaota* phylum (*Nitrosopumilus* genus) (Curtis-Harper et al., 2018) (Table 2).

The microbial enrichment was prepared by adding 5 g of dry sediment to an anaerobic enrichment medium containing per litre: 2 g of trypticase peptone (Sigma Aldrich), 2 g of yeast extract (Sigma), 0.3 g of KCl, 1 g of NH_4Cl, 3 g of Na_2SO_4, 23 g of NaCl, 0.5 g of Na-Lactate, 2 g of $MgCl_2$, 0.35 g of K_2HPO_4, 0.1 g of Na-thioglycollate ($C_2H_3NaO_2S$) and 0.1 g of ascorbic acid ($C_6H_8O_6$), and was prepared anaerobically, as previously described (Hungate, 1966). Vitamin solution (Balch et al., 1979) and SL10 trace element solution (Widdel et al., 1983) were added post-autoclaving (121°C, 15 psi, 15 min). 100 ml of medium was aseptically transferred (under anaerobic conditions) to sterilised Wheaton bottles (Speers et al., 2009), and after inoculation, the headspace was pressured to 2 bar with 80% CO_2/20% H_2. The cultures were incubated at 14°C, for 700 h (29 days), and subsequently transferred twice to eliminate any crossover from the sediment.

2.3 Dissolution experiments

The dissolution experiments were conducted with a $(W/R)_E$ of 100/33 (we denote W/R_E as the experimental water to rock ratio and denotes the amount of rock and the amount of water) with a nutrient-limited anaerobic minimal medium, which contained the following (per litre): 1 g of NH_4Cl, 2 g of Na-lactate ($C_3H_5NaO_3$), 1 g of Na-thioglycollate ($C_2H_3NaO_2S$), 1 g of ascorbic acid ($C_6H_8O_6$), 37 g of NaCl, 13.25 g of Na_2CO_3. To prepare the regolith simulant, 8.09 g of basalt and 5.91 g of aegirine were dispensed into acid-washed Wheaton bottles, which had been purged with N_2 to remove O_2. The regolith was autoclaved at 121 C for 15 min and after cooling, 68 ml of medium was added, and the pH was adjusted to pH 7.0 with filtered sterilised 10 mM NaOH. For the inoculum, exponential phase cells were harvested by centrifugation (4,000 × *g*, for 5 min), washed, and resuspended in the minimal medium to give a final cell density of 10^7 to 10^8 cell mL^{-1}. A 1% inoculum was used for the biotic experiments (designated V1, V2, V3, V4 and V5) and abiotic controls were prepared in parallel (designated VA1, VA2, VA3, VA4 and VA5). The headspace of all of the Wheaton bottles were overpressured to 2 bar with 80% CO_2/20% H_2, prior to incubating at 15 C for 700 h. Microbial growth was measured every 24–48 h over the course of the 29 days experiment (closed system simulation) using the acid-binding Sybr, as previously described by Olsson-Francis et al. (2017). The duration of the dissolution experiment was also dictated by the experimental design (closed system simulation) that limited the availability of nutrients for microbes and by the fact that, interrupting the experiments after 700 h (point at which the microbial community reached the stationary phase), it was avoided a reduction in abundance and diversity of microbes relating to the selection of specific metabolic groups. To monitor microbial growth in absence of the regolith simulant, experiment controls were also performed combining the microbial community and the minimal medium only. In such cases, no microbial growth was observed; for this reason, this aspect will not be further discussed.

2.4 Chemical analyses of the medium

An Orion 3-Star Thermo Scientific bench top meter with an uncertainty of 0.01 pH unit was used to measure the pH of the media. A Prodigy High Dispersion Inductively Coupled Plasma-Atomic Emission Spectrometer (ICP-AES) was used to measure the total elemental concentration of dissolved elements in the medium. In triplicates, 1 ml aliquots were removed aseptically from each Wheaton bottle after 700 h. The aliquots were centrifuged at 400 × *g*, for 2 min to eliminate any residual regolith simulant from the analytical sample, and then acidified using nitric acid (10%). Detection limits for the ICP-AES were defined as 3 times above blank level. The ICP-AES data were corrected for the loss of elemental mass during sampling and for the decrease in fluid volume, as described in Wu et al. (2007).

2.5 Cellular elemental uptake

To measure the intracellular elemental concentration, 1 ml aliquots were centrifugated (4,000 × *g* for 2 min) and the supernatant collected (to remove any excess regolith). The cells were harvested and washed three times in sterilised 0.5% HNO_3 by centrifugation (13,000 × *g* for 10 min) to remove excess media. The cells were acidified by resuspending the cells in 10% nitric acid. This allowed the elemental content of the cells to be measured using a Prodigy High Dispersion Inductively Coupled Plasma Atomic Emission Spectrometer (ICP-AES). The values obtained were multiplied by the number of cells measured at

TABLE 3 Composition of the fluid used in the models.

Ion	Concentration (moles)
H^+	0.2357
O_2	0.4802
Cl^-	0.6518
S^-	0.0088
C	0.2302
Na^+	0.9097
N^+	0.0187

Species in the fluid are summarized in the table as one species, but during the modelling were partitioned into several dissolved species.

700 h and were corrected for the decrease in fluid volume during sampling, as previously described (Wu et al., 2007; Olsson-Francis et al., 2012).

2.6 Characterization of the simulant after dissolution experiments

After 700 h, the regolith simulant was removed from the Wheaton bottle, air-dried, and carbon coated (15–20 μm thickness) on aluminium stubs. The chemical composition and the morphological characteristics of the simulant were determined using a ZEISS Supra 55-VP Field Emission Gun - Secondary Emission Microscope (FEG-SEM) with an Energy Dispersive Spectroscopy (EDS) detector, which was operated at an accelerating voltage of 2–15 kV and a 7–10 mm working distance. Secondary electron images, backscatter electron images and EDS spectra obtained from FEG-SEM analysis were compared and used to identify the presence of secondary minerals that may be used as bio-signatures.

2.7 Thermochemical modelling

Thermochemical models were executed to identify reaction pathways, shifts in fluid chemistry and mineral formation that would occur over geological timescales under biotic and abiotic conditions in the considered fluid-rock systems. The code CHIM-XPT (previously CHILLER, Reed and Spycher, 2006; Reed et al., 2010) was used to perform stepwise titration simulations during which a specific amount of rock was titrated into a constant amount (1 L) of the starting fluid. The model assumes complete rock dissolution and each titration step is in equilibrium, and therefore can be interpreted independently. The reaction progress is expressed as water to rock ratio (W/R), which represents the amount of rock reacted with the fluid. By modelling at different $(W/R)_M$ (water to rock ratio used in the models), the software simulates chemical reactions that may happen under different environmental conditions (e.g. Reed, 1982; Filiberto and Schwenzer, 2013; Bridges et al., 2015). At very high W/R (~1,000,000), the model simulates an environment where a limited amount of rock react with a large mass of water (e.g., freshwater inflow, fluid percolating in a fracture, a rock surface exposed to regular precipitation), while at low W/R ratios (<1,000), the model represents a scenario where a large volume of rock reacts with a limited volume of water (e.g., stagnant water table like in lacustrine-sediment settings). More information on the code and method and its application and limitations can be found in Palandri and Reed (2004), Reed and Spycher (2006) and Reed et al. (2010).

The input data for the thermochemical modelling included the Mars regolith simulant composition (Table 1) and the chemical composition of the minimal medium (Table 3). Elements in the fluid summarised in Table 3 are given as component species and in the model calculation partitioned between several species as relevant to the pH and Eh conditions during the modeling. The code applies mass balance and mass action equations to calculate the equilibrium of secondary alteration mineral assemblages and fluid composition at different water/rock ratios. The modelling was carried out at 2 bar and 14°C, which was used to simulate the pressure and temperature conditions of the growth experiment. The models were run over a range of $(W/R)_M$ ratios between 10^5 and 1. Three models were conducted: in the first, the pH was allowed to vary and was treated as a free parameter to simulate rock weathering in an abiotic environment. In the other two models, the pH was set at 7.0 and 7.4 to reproduce the minimum and maximum pH conditions observed during microbial growth experiments simulating weathering progression in presence of the considered bacterial community. Full data tables, minerals suppressed in the modelling because not stable at low P and T conditions (2 bar, 14 C) or not forming in the simulated Martian environment and relative references are presented in Supplementary Material.

3 Results

3.1 Microbial growth

The microbial community grew in the minimal medium with the Mars regolith simulant as the sole source of bio-essential elements. Exponential growth occurred between 24 h ($1–5\times10^5$ cells mL^{-1}) and 300 h ($4–7 \times 10^6$ cells mL^{-1}) after inoculation (Figure 1). After 300 h, the cultures reached stationary phase and cells numbers remained relatively constant between 5 and 6×10^6 cells mL^{-1} (Figure 1). No growth was detected in the abiotic controls.

In the biotic controls, the mean pH increased from 7.07 ± 0.08 to 7.36 ± 0.06 in the first 170 h and then stabilised to 7.29 ± 0.02 until the end of the experiments (Figure 1A, Supplementary

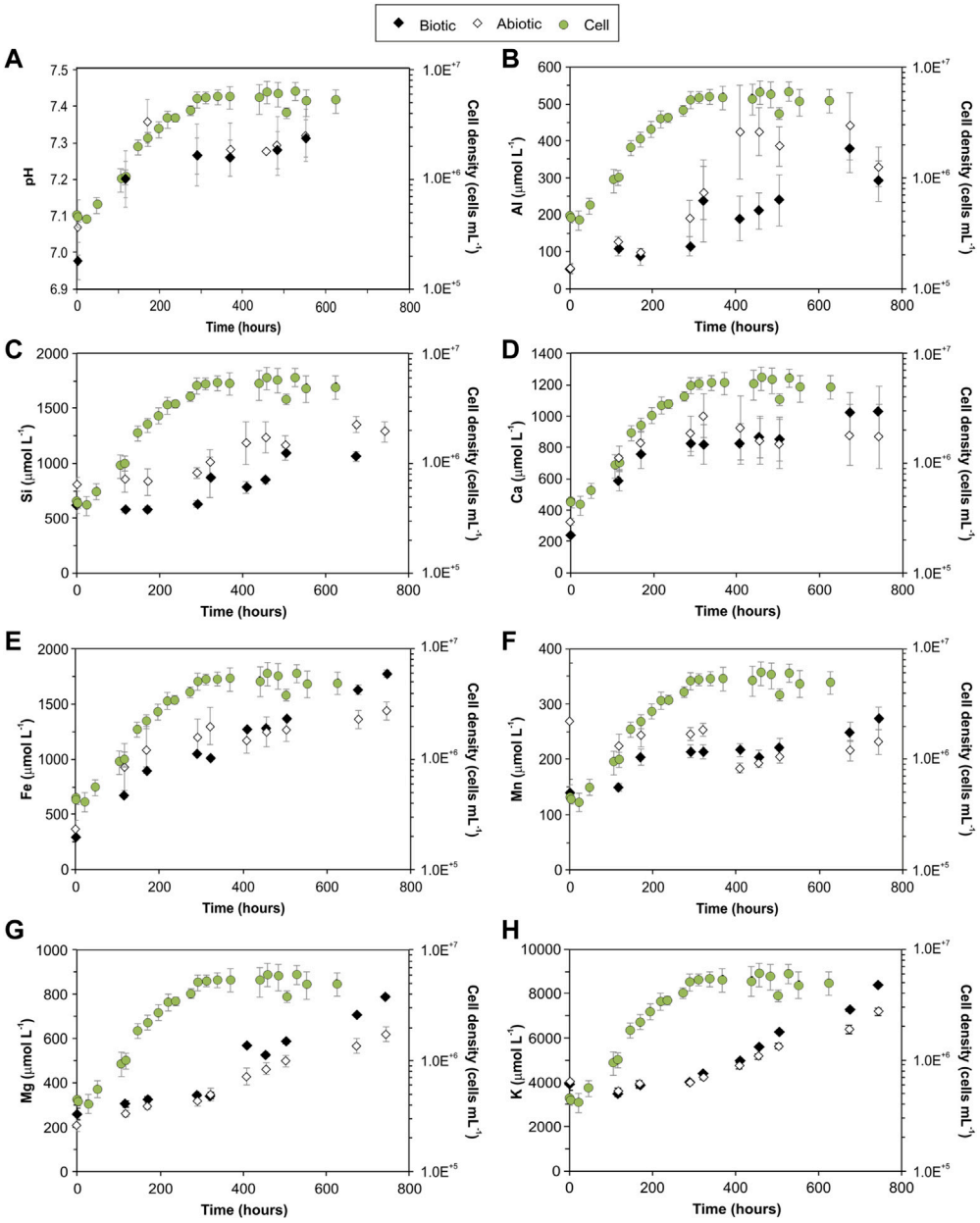

FIGURE 1
Mean pH value of the medium **(A)** and mean concentration of elements in the medium **(B–H)** over the course of biotic and abiotic experiments, plotted in parallel to the logarithmic plot of cell density. Error bars represent the standard error of the mean for all series. Full data are listed in Supplementary Material.

Material). For the abiotic controls, the pH increased from 6.98 ± 0.08 to 7.31 ± 0.08 (Figure 1A, Supplementary Material).

3.2 Regolith simulant dissolution

Simulant dissolution was measured by the concentration of key rock forming elements (Si, K, Ca, Mn, Mg, Al and Fe) released into the medium (Figures 1B–H, Supplementary Material). The elemental concentrations in the fluid increased over time in both abiotic and biotic experiments. For the duration of the experiments, dissolved Si and Al had higher concentrations in the abiotic controls than the biotic experiments; Mg was higher in the biotic experiments, as shown in Figure 1G, with a minimum and maximum difference of ~30 $\mu molL^{-1}$ and ~170 $\mu molL^{-1}$, respectively,

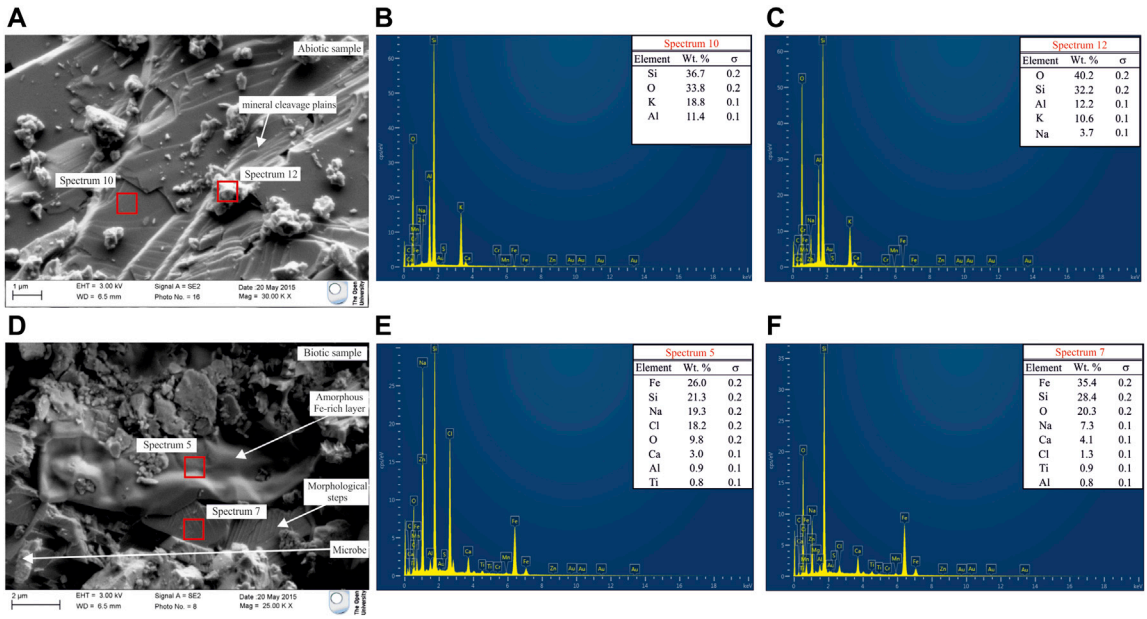

FIGURE 2
(A) FEG-SEM micrograph of the simulant after the abiotic experiment. Minimal alteration was observed along cleavage plains; **(B)** EDS spectrum of a mineral in the abiotic control; **(C)** EDS spectrum of a Na-enriched grains on top of the mineral. Na enrichment happened during sample drying before sample preparation; **(D)** FEG-SEM micrograph of the simulant after the biotic experiment. An amorphous layer on the surface of some crystals is evident; **(E)** EDS spectrum of the amorphous layer; **(F)** EDS spectrum of the mineral beneath the amorphous layer.

between the biotic and abiotic controls. The microbial growth phase influenced the dissolution of certain elements, e.g., after 300 h (exponential growth), K was higher under biotic conditions, and the concentrations of Fe, Ca and Mn were higher in the biotic experiments than the abiotic experiments only during the late stationary phase (>400–500 h).

3.3 Secondary alteration minerals

FEG-SEM with EDS was used to investigate secondary alteration products (secondary minerals, amorphous phases) formation and morphological changes on the surface of the simulant. Analysis of the abiotic samples demonstrated that the mineral surfaces showed little or no evidence of physical or chemical weathering (Figures 2A–C). Analysis of the regolith simulant from the biotic experiments showed some microbial attachment and evidence of chemical and physical changes on the mineral surfaces (Figures 2D–F). This included morphological steps observed along mineral cleavage plains and amorphous layers with smooth, rounded and undulate surfaces observed on top of some weathered grains (Figure 2D). SEM-EDS analysis demonstrated that the amorphous layers were mainly composed of Fe, Si, O and Na with lower amounts of Cl, Ca and Al (Figures 2E,F).

3.4 Thermochemical modelling

Figures 3, 4 show the changes in mineralogy and fluid compositions that would occur over geologically timescales under biotic and abiotic conditions as the weathering reactions advance and the $(W/R)_M$ ratios decrease from 10^5 to 1. Table 4 shows all the minerals that precipitate in the abiotic and biotic models at different $(W/R)_M$ ratios. Variation in element concentration in the fluid that are not directly comparable with data from dissolution experiments but that are relevant for secondary minerals formation predicted by the models are reported in Supplementary Material.

3.4.1 Abiotic model

The abiotic model (Figure 3A) forms the baseline from which to compare the biotic models. From high to low $(W/R)_M$ ratios the secondary mineral assemblage became more complex. Pyrite formed at $(W/R)_M$ ratio of 10^5, which was stable over the considered $(W/R)_M$ ratio range, and progressively decreased from 100 wt% to <1 wt%. This reduction in pyrite coincided with other Fe-rich minerals forming and the $(W/R)_M$ ratio decreasing. Talc formed below a $(W/R)_M$ ratio of 100,000, it reached its maximum abundance (~21 wt%) at a $(W/R)_M$ ratio of 3,330 when quartz started to form. The values remained constant between 12 wt % and 16 wt% up to a $(W/R)_M$ ratio of 1. Between $(W/R)_M$

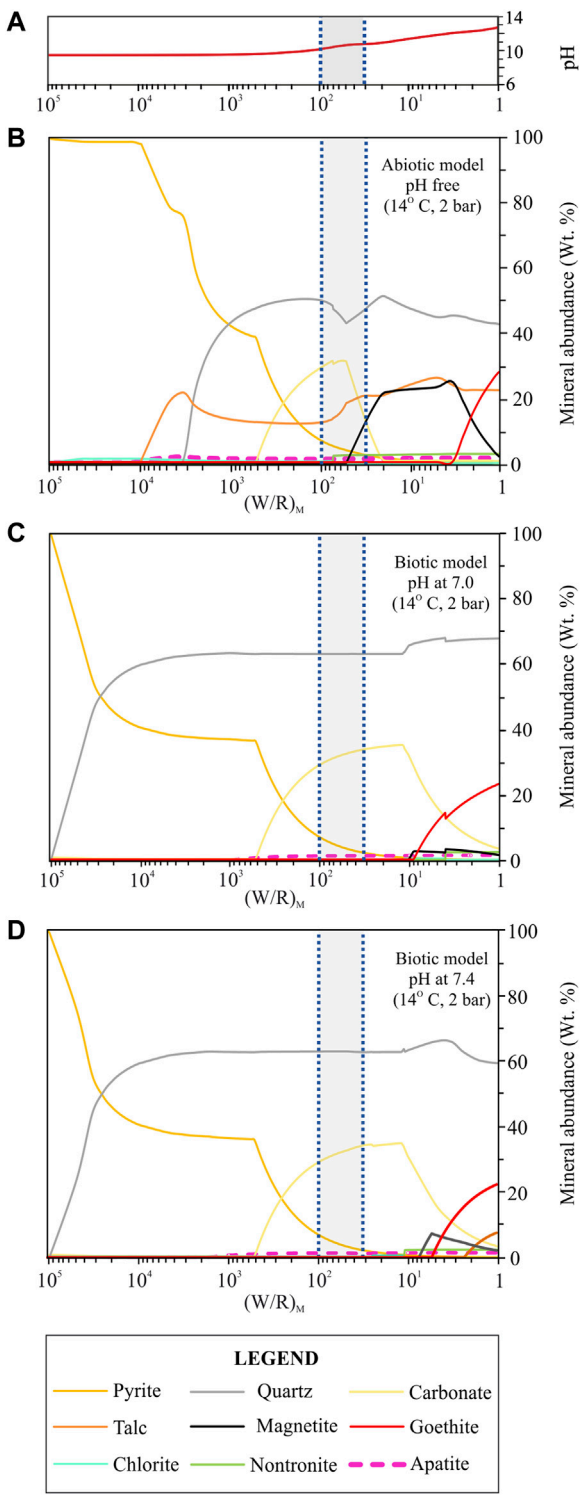

FIGURE 3
Secondary minerals predicted from the dissolution of the regolith simulant at 14°C and 2 bar under abiotic and biotic conditions. **(A)** variation of the pH in the abiotic model; **(B)** abiotic model where the pH was set as a free parameter; **(C)** biotic model where the pH was set at 7.0; **(D)** biotic model where the pH was set at 7.4. The diagrams show the formation of pyrite, quartz, carbonate, talc, magnetite, goethite in different amounts and traces of chlorite, nontronite, apatite and kaolinite (not shown in the diagram since its abundance is <<1 wt%). For more details on the variability of the minor phases (chlorite, nontronite, apatite and kaolinite) see supplementary materials A, B, C. The $(W/R)_D$ is represented by the shadowed area in between the two blue dotted vertical lines and it was calculated based on the element potassium because it is not incorporated into the microbes and into any of the expected mineral precipitates.

ratio of 3,300 and 500, pyrite (75–40 wt%), quartz (20–47 wt %), and talc (~21—12 wt%) were the main precipitates. Siderite, which formed at $(W/R)_M$ ratio of 500 together with trace amounts of Fe-talc, reached a maximum abundance of ~31 wt%, at a $(W/R)_M$ ratio of 55 and was no longer stable below a $(W/R)_M$ ratio of 20. Siderite coexisted with quartz (~42–50 wt%), pyrite (<2–37 wt%), talc (12–14 wt %), Fe-talc (<1–6 wt%) and, below a $(W/R)_M$ ratio of 50, magnetite (<5–21 wt%). Between $(W/R)_M$ ratios of 20 and 3, only minor variations (<5 wt%) in the abundance of quartz, magnetite, talc, Fe-talc and pyrite were observed. Magnetite reached its maximum abundance of 25 wt% at a $(W/R)_M$ ratio of 3. Below this threshold, magnetite declined to 2 wt%, while goethite started to form (8–27 wt%). Chlorite (clinochlore, daphnite, Mn-chlorite), carbonates (rhodochrosite), Na- and K-nontronite and hydroxyapatite also formed in trace amounts (<3 wt%) at various $(W/R)_M$ ratios.

The pH of the fluid varied between 9.5 and 12.7 over the course of the titration range (Figure 4A, Supplementary Material). The concentration of most of the dissolved elements and component species varied by, at least, two orders of magnitude except for Cl^-, HS^-, NH_4^+, Na^+ and HCO_3^-, which were more stable and less variable (Figure 4B, Supplementary Material). The concentration of abundance of Mg^{2+}, Ca^{2+} and Al^{3+} generally decreased, while the amount of HPO_4, H_4SiO_4, Mn^{2+}, K^+ and Fe^{2+} generally increased (Figure 4B, Supplementary Material). Al^{3+} and Fe^{2+} were the most variable elements and showed more complex patterns (Figure 4B, Supplementary Material) that can be associated with the formation of variable amounts of Al- and Fe-rich phases in the considered titration range.

3.4.2 Biotic models

When the pH was set at 7.0 and 7.4 (simulating the small change in the buffered medium), the models (Figures 3C,D) gave similar results in terms of secondary mineral assemblages and fluid chemistries. Pyrite was stable over the considered $(W/R)_M$ ratio range with its abundance progressively decreasing from 100 wt% to <1 wt% when quartz started to form ($(W/R)_M$ ratio of ~100,000). Below this value, quartz increased and was the most abundant mineral phase at a $(W/R)_M$ ratio lower than 25,000 (a maximum value of 67 wt% was measured at end of the titration range).

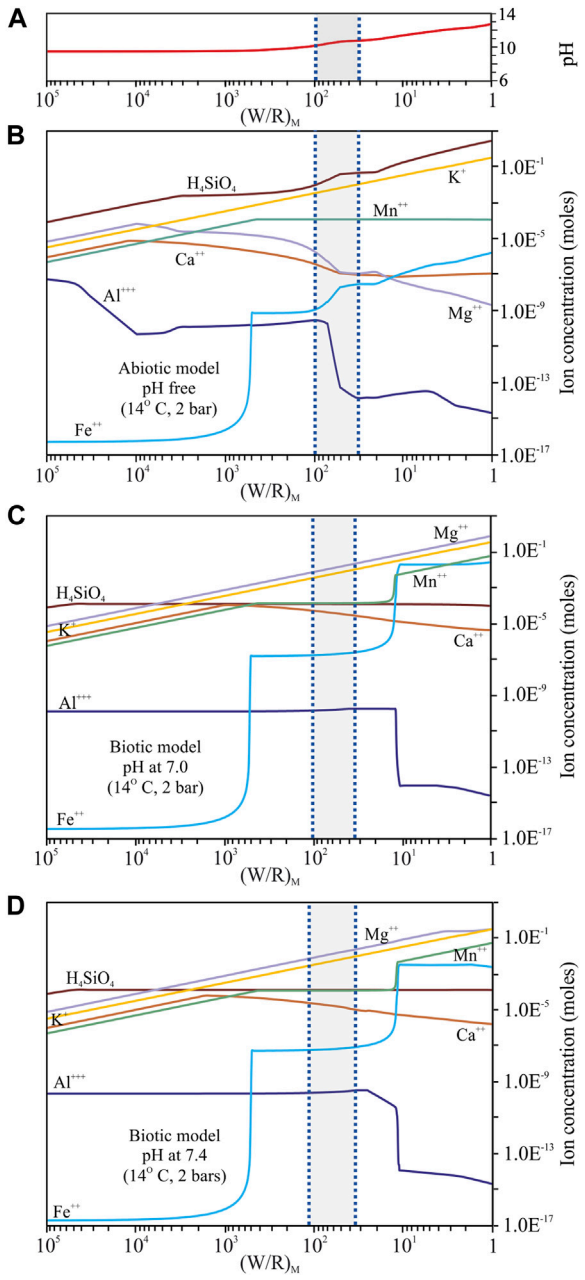

FIGURE 4
Fluid composition predicted from the dissolution of the regolith simulant at 14°C and 2 bar. **(A)** pH variability in the abiotic model; **(B)** model with pH as a free parameter that varies between 9.5 and 12.7; **(C)** model with pH set at 7.0; **(D)** model with pH set at 7.4. Only elements relevant for a direct comparison between the models and the basalt dissolution experiments are shown in the diagrams (H_4SiO_4, Mg^{2+}, Mn^{2+}, K^+, Ca^+, Al^{3+}, Fe^{2+}). For more details on the variability of the other elements (Cl^-, HS^-, NH_4^+, Na^+, HCO_3^-, HPO_4) see supplementary materials A, B, C. The $(W/R)_D$ is represented by the shadowed area in between the two blue dotted vertical lines and it was calculated based on the element potassium because it is not incorporated into the microbes and into any of the expected mineral precipitates.

When the pH was fixed at 7.4, quartz reached its maximum abundance of 68.8 wt% at a $(W/R)_M$ ratio of ~3. Quartz and pyrite were the major phases that formed between $(W/R)_M$ ratios of 100,000 and 500. Siderite precipitated only below a $(W/R)_M$ ratio of 500, together with quartz (~62–65 wt%) and pyrite (~35–< 1 wt%). Siderite increased up to ~34 wt% at a $(W/R)_M$ ratio of 11, and then started to decline. Below a $(W/R)_M$ ratio of 10, quartz continued to be stable with a maximum abundance of ~69 wt%, siderite decreased from 34 wt% to <3 wt%, and goethite reached its maximum concentration of around 22 wt% at $(W/R)_M$ ratio of 1. Below $(W/R)_M$ of 10, magnetite formed (<4 wt%) when the pH was set at 7.0, while it reached 7 wt% when the pH was set at 7.4. Huntite formed in traces (<1 wt%) only when the pH was set at 7.4 and between $(W/R)_M$ ratios of 50 and 24; whilst talc (<7.5 wt%) formed only when the pH was set at 7.4 below a $(W/R)_M$ of 3. Trace amounts (<1–3 wt%) of chlorite (clinochlore, daphnite), carbonates (rhodochrosite), kaolinite, nontronite and hydroxyapatite were also formed at different $(W/R)_M$ ratios.

Most of the dissolved elements, here given as component species, varied in concentration by, at least, one order of magnitude with the exception of Cl^-, H_4SiO_4, $NH_4^+$and Na^+ that were relatively stable (Figures 4C,D, Supplementary Material). HPO_4, Mg^{2+}, Mn^{2+} and K^+ steadily increased, while Ca^{2+} increased up to a $(W/R)_M$ ratio of ~1,000 and then decreased in concentration; HS^- and HCO_3^- decreased only at a $(W/R)_M$ ratio below 10 (Figures 4C,D, Supplementary Material); Al^{3+} decreased by five orders of magnitude below a $(W/R)_M$ ratio of 10 because it precipitates in Al-rich phases (chlorites) that form at the end of the $(W/R)_M$ ratio range (Figures 4C,D, Supplementary Material). Fe^{2+} showed a more complex pattern and a variation of more than 10 orders of magnitude between $(W/R)_M$ ratio of ~1,000 and ~1 (Figures 4C,D, Supplementary Material); this is correlated with the different amounts of Fe-rich minerals that formed in the considered $(W/R)_M$ ratio range.

4 Discussion

4.1 Experimental regolith simulant dissolution

In this study, variations in fluid chemistry, as well as mineralogical and morphological changes to a Martian regolith simulant, were investigated to identify inorganic bio-signatures produced by chemolithotrophic and chemoorganoheterotrophic microbes, which might be detected in the Martian rock-record and which might be analogue to those that may have lived in the fluvio-lacustrine system at Gale Crater on early Mars (e.g. Curtis-Harper et al., 2018).

TABLE 4 List of minerals that form in abiotic and biotic models at 14°C, 2 bar between $(W/R)_M$ of 10^6 and 1.

Mineral	Formula	Abiotic model	Biotic model (pH 7.0)	Biotic model (pH 7.4)
pyrite	FeS_2	X	X	X
quartz	SiO_2	X	X	X
Hydroxy apatite	$Ca_5(PO_4)_3OH$	X	X	X
siderite	$FeCO_3$	X	X	X
rhodochrosite	$MnCO_3$	X	X	X
clinochlore	$Mg_5Al_2Si_3O_{10}(OH)_8$	X		X
daphnite	$Fe_5Al_2Si_3O_{10}(OH)_8$	X	X	X
Mn-chlorite	$Mn_5Al_2Si_3O_{10}(OH)_8$	X		
Na-nontronite	$Na_{0.3}Fe_2$ $[(Si,Al)_4O_{10}]$ $(OH)_2{\cdot}nH_2O$	X	X	X
K-nontronite	KFe_2 $[(Si,Al)_4O_{10}]$ $(OH)_2{\cdot}nH_2O$	X	X	X
talc	$Mg_3Si_4O_{10}(OH)_2$	X		X
Fe-talc	$Fe_3Si_4O_{10}(OH)_2$	X		
magnetite	Fe_3O_4	X	X	X
goethite	$FeO(OH)$	X	X	X
kaolinite	$Al_2Si_2O_5(OH)_4$		X	
huntite	$Mg_3Ca(CO_3)_4$			X

ICP-AES analysis detected specific changes in the fluid chemistries that differed between the biotic and abiotic test groups, e.g., microbial mediated dissolution increased the dissolved concentrations of Mg, Fe, Mn, Ca and K. Previous studies demonstrated that excess protons and low molecular weight organic acids, produced as a by-product of microbial metabolism, can alter the pH of the fluid promoting the extraction of bio-essential elements from rocks (Vandevivere et al., 1994; Liermann et al., 2000; Huston and Logan, 2004; Wu et al., 2007) and the formation of secondary alteration minerals (Banfield et al., 2001; Berg et al., 2020). In our study, changes in element concentration could not be solely ascribed to the pH differences between the abiotic and biotic experiments. Given that the pH of the media remained nearly neutral during biotic experiments because of the buffering capacity of the simulant, it is possible that organic acids may have enhanced mineral dissolution locally, e.g. in pore spaces and close to mineral surfaces, without changing the pH of the whole system. Micro-reaction zones have previously been identified at microbial binding sites and are associated with high concentrations of organic acids (Hiebert and Bennett, 1992; Thorseth et al., 1992; Vandevivere et al., 1994). Although there is little evidence of direct microbial attachment to the mineral surface it is still possible that elemental dissolution in the biotic experiments has occurred through direct contact of the microbes with the simulant, and also indirectly (Hiebert and Bennett, 1992; Vandevivere et al., 1994; Banfield et al., 2001; Welch et al., 2002; Konhauser, 2007; Lian et al., 2008; Uroz et al., 2009; Gadd, 2010). Differences between the amount of element dissolved in the fluid in this study and previous studies (Wu et al., 2007; Olsson-Francis et al., 2017) could be explained by the inclusion of a buffer in the system that may have prevented elemental release as a result of high pH changes, or the use of a more complex microbial community instead of a single microbe type (*Burkholderia sp. strain B_33*—Olsson-Francis et al., 2017; *Burkholderia fungorum* - Wu et al., 2007). Heterotrophic microorganisms, such as *Burkholderia fungorum*, use organic compounds as source of energy and chemical equilibrium is more easily reached and dissolution is at minimum (Wu et al., 2007). In a mixed community, that contains also chemolithotroph microorganisms which require chemical compounds and elements (sourced from the fluid and the rock) to produce energy, dissolution rates increase due to the pH being far from equilibrium (Ramkissoon et al., 2021).

Morphological steps observed along mineral cleavage plains and Fe-Si rich amorphous deposits (Figure 2D) identified by SEM on the surfaces of some aegirine grains in the biotic experiments are, respectively, evidence of enhanced mineral weathering and secondary mineral deposition following microbial action (Brantley and Chen, 1995; Benzerara et al., 2004; Benzerara et al., 2005; Wu et al., 2007). According to the elemental distribution in "spectrum 5" (Figure 2E), the amorphous deposit may represent partially dissolved aegirine and the formation of non-crystalline Fe-rich secondary clay at the mineral surface, characteristic of an early stage of pyroxene weathering (Nahon and Colin, 1982). We interpret this as evidence for mineralogical changes specific to the biotic experiments as nothing comparable was observed in the abiotic experiments. Peaks detected for Ca, Na and Cl are interpreted as $CaCl_2$ and NaCl deposits precipitated on top of the Fe-Si rich amorphous layer during sample drying before SEM analysis.

Previous studies that used a naturally occurring, already altered, basalt as a Martian analogue observed similarities between secondary minerals formed during biotic laboratory experiments and those predicted by thermochemical models (Olsson-Francis et al., 2017). In our study, mineralogical features observed in the biotic samples and alteration phases predicted by biotic models are not directly comparable, as detailed analyses of secondary mineralisation formed experimentally were limited by the rarity of potential secondary minerals at detectable abundances. The use of an unweathered fresh basalt, of a small grain size (<250 μm) and the short duration of the experiments could have reduced the likelihood of alteration phase formation in our study, impeding a comparison with model results. Longer experimental run times in a simulated open-system environment would be needed to observe the development of a more complex alteration assemblage, the formation of larger quantities of secondary minerals and more pronounced alteration features that would be more easily detectable, and thus comparable with secondary minerals predicted by the biotic and abiotic models.

4.2 Thermochemical models of basalt dissolution

Thermochemical modelling was used to assist in the identification of possible inorganic bio-signatures, such as secondary alteration minerals and fluid chemistry variations, that form during microbial weathering of the Martian simulant over geological timescales in an aqueous system. To compare the experimental and model results, we focus on a specific $(W/R)_M$ range, between 100 and 38 (Figures 3, 4), that is equivalent to the actual $(W/R)_D$ ratio interval of the growth experiments. The $(W/R)_D$ ratio is defined as the amount of regolith dissolved during the experiments; it was assessed by focusing on the most soluble elements (e.g. K^+) in the fluids resulting from the experiments and calculated as outlined in Olsson-Francis et al. (2017). K^+ was specifically selected because it is not incorporated into microbial cells or (in large amounts) into any of the minerals predicted to precipitate by the models (see Results section). The $(W/R)_M$ ratio range considered here (between 100 and 38) is also equivalent to a lacustrine-sedimentary setting where a limited amount of water interacts with a large volume of rock. As described in detail earlier, similar environments have been identified by rover missions at Gale and Jezero Craters (Grotzinger et al., 2014; Vaniman et al., 2014; Mangold et al., 2021) and are proposed as sites that could have supported microbial life in early Martian's history (Rampe et al., 2020).

Under lacustrine-sedimentary conditions, a less complex secondary mineral assemblage forms during biotic dissolution compared to abiotic, where more mineral species precipitate (Figure 3). The models show that under biologically-mediated conditions, high amounts of quartz and carbonates (mainly siderite, but also traces of rhodochrosite and huntite) coexist with minor amounts of Fe-sulfides (pyrite) and trace amounts of phosphates (hydroxyapatite), whereas the abiotic system would also precipitate Fe-oxides (magnetite) and various amounts of phyllosilicate minerals (talc, chlorites, nontronite). Less chemically and mineralogically complex secondary mineral assemblages seem to be common features of basalt-fluid interactions under biotic conditions at 1 bar and temperature ≤25 C (Olsson-Francis et al., 2017), well below the threshold at which life can exist (<121°C, e.g., Conrad, 2014; Cockell et al., 2016).

The differences in the fluid compositions between an abiotic and a biotic environment are more pronounced in the models, where rock dissolution is simulated for longer periods of time (e.g., geological timescales), than in laboratory experiments which investigate rock alteration only for a few weeks. Within the considered $(W/R)_M$ ratio range between 100 and 38, that simulates lacustrine-sedimentary conditions, K, Si and Mn were observed in similar concentrations (10^{-3} mol, 10^{-4}°mol and 10^{-4}°mol, respectively) in the biotic models as in the growth experiments (Figures 1, 4, Supplementary Material), suggesting that these elements are used by the microbes only in minimal amounts and that their behaviour is similar during short- and long-term biotic weathering. This is also supported by the fact that the cellular elemental uptake measured after biotic experiments was below the detection limits (Supplementary Material). Mg remains lower in the experimental fluid compared to model results. This could be related to microbial activity that impedes elemental dissolution by producing amorphous layers on top of some minerals (e.g., pyroxene) (Benzerara et al., 2004; Benzerara et al., 2005), promoting adsorption of polysaccharides onto mineral surfaces (Welch et al., 1999), producing high-molecular-weight polymers (Welch and Vandevivere, 1994) and preventing the formation of etch-pits (Lüttge and Conrad, 2004). According to model results, Mg would not precipitate in large amounts in secondary minerals predicted to form under biotic conditions, and it would accumulate in the fluid during long-term regolith alteration. Fe, Ca and Al contents were higher in the experimental fluids than in the modelled fluids, suggesting that biological activity is a limiting factor for precipitation of these elements during short-term weathering.

Inhibition of precipitation could be related to different processes associated to specific biological functions. Microbes take up specific bio-essential elements (oxygen or phosphate) to form inorganic or organic compounds, including proteins and siderophores, that are used for internal vital processes; the production of polysaccharides and other extracellular polymeric substances is another way of how microbes can attract and use bio-essential elements for their external functions; finally, microbes also use various chemicals to produce and release organic compounds such as low

molecular weight organic acids (Welch and Ullman, 1993; Vandevivere et al., 1994; Barker and Banfield, 1998; Kalinowski et al., 2000; Bennet et al., 2001; Wu et al., 2007; Uroz et al., 2009; Gadd, 2010; Olsson-Francis et al., 2015). These processes would prevent solubility limits being reached, impeding the precipitation of secondary minerals that could form in the considered water-rock system during long-term dissolution. As predicted by the models, these phases could be pyrite (FeS_2), siderite ($FeCO_3$), hydroxyapatite ($Ca_5(PO_4)_3OH$) and Al-rich minerals (kaolinite, $Al_2SiO_5(OH)_4$).

4.3 Alteration minerals and life detection on Mars

Fe-phyllosilicates (nontronite and chlorite) and Fe-oxide (magnetite), predicted by thermochemical modelling to form only under abiotic conditions, have been found at several sites on Mars (Ehlmann et al., 2009; Carter et al., 2013; Ehlmann and Edwards, 2014; Rampe et al., 2020). Chlorite is an uncommon alteration mineral at very low-temperature since it forms preferentially in diagenetic and low-temperature metamorphic environments. However, it is thought to be authigenic in weathered sedimentary deltaic sandstones at 20–40 C (Grigsby, 2001) and has been found widespread on Mars (Ehlmann et al., 2011). Talc is also predicted by the abiotic model to form but its presence on Mars is still uncertain (Bristow et al., 2021). Talc is usually associated to higher temperature regimes (hydrothermal alteration) and metamorphic conditions; however, talc can be also authigenic in sedimentary deposit (Tosca et al., 2011 and references therein) or, as demonstrated in laboratory test performed at ambient conditions, it can precipitate as a secondary product in low-temperature aqueous systems as a precursor of Mg-rich carbonate deposits (Bricker et al., 1973; Tosca et al., 2011). In all these cases, talc precipitation seems strongly controlled by the pH and favoured under alkaline conditions (Tosca et al., 2011). Carbonate minerals (e.g., siderite and rhodochrosite) characteristic of both biotic and abiotic models have been observed in Martian meteorites (e.g., nakhlites, Changela and Bridges 2011; Melwani Daswani et al., 2016; Bridges et al., 2019) and by orbiting spacecraft and rovers on the Martian surface at various locations (e.g., Gale and Jezero Craters, Bultel et al., 2019; Bridges et al., 2019; Thorpe et al., 2020; Archer et al., 2020; Horgan et al., 2020). Other alteration minerals predicted to form under biotic and abiotic conditions such as quartz, pyrite and hydroxyapatite have also been discovered (Vaniman et al., 2014; Rampe et al., 2020). The carbonates huntite, which precipitates in trace amounts only in the biotic model at pH of 7.4, has not been directly observed on Mars, although it has been inferred to occur in Nili Fossae region (Palomba et al., 2009). However, since it can form at surface temperatures and pressures in fluvial-lacustrine evaporitic environments or as an alteration mineral in basalts weathered by cold solutions rich in Mg, Ca and carbonic acid (Kinsman 1967; Cole and Lancucki, 1975; Stanger and Neal, 1994; Akbulut and Kadir, 2003), it is likely to be present in ancient Martian systems similar to Gale and Jezero Craters. Huntite, could be particularly difficult to detect on Mars (especially if present in low amounts) since it is metastable at surface temperature (Garrels et al., 1960; Kinsman, 1967) and it is replaced with time by magnesite (Kinsman, 1967; Spotl and Burns, 1994; Marini, 2007), a more stable Mg-carbonate that is present on the Martian ground together with siderite, calcite, rhodochrosite and other Mg- and Fe-bearing alteration minerals (Ehlmann et al., 2008; Niles et al., 2013; Goudge et al., 2015). Finally, alteration phases predicted to form in the biotic system (siderite, rhodochrosite, quartz, pyrite, hydroxyapatite) are all minerals that naturally can precipitate in near-neutral pH aqueous environments at ambient temperature following the action of microbes (Lee et al., 2007; Ehrlich and Newman, 2009; Sun et al., 2014; Duverger et al., 2020).

The results of this study provide indications of which mineralogical and geochemical features need to be investigated when searching for inorganic bio-signature on Mars. Alteration effects and mineral deposits of such small scale (<15 μm) would be difficult, if not impossible, to be observed *in-situ* using the instruments on board of Martian rovers (Mars Hand Lens Imager instrument aboard Curiosity rover has a resolution up to 13.9 microns/pixel) (e.g. Edgett et al., 2012; Allwood et al., 2020). However, such information and observations are relevant for searching for the most likely sites to find putative life. The chemical changes associated with the observations in this study, while not resolved in the detail required to analyse them, might still be indicated through gradients and deviations from baseline mineral observations in spatially resolved techniques such as the Planetary Instrument for X-Ray Lithochemistry (PIXL) on Perseverance (Allwood et al., 2020). Moreover, a complex mineralogical assemblage and secondary minerals large enough to be detected by rovers' instruments are likely to have been formed in a natural Martian environment where the interaction between the substrate and the microbes, if ever been present, would have been prolonged over longer periods. Therefore, the results of this study are required for potentially informing the current sampling activities operated by the Perseverance rover, for planning future life detection missions and for interpreting the results of the analysis of Martian samples recovered by future sample return missions.

5 Conclusion

In this study, laboratory-based experiments and thermochemical modelling were combined to investigate inorganic bio-signatures formed by an analogue microbial community from an anoxic inter-tidal zone of a Martian analogue fluvio-lacustrine system and that could be used as

evidence in the search for life in early Martian lacustrine-sedimentary systems. Analogue microorganisms used in dissolution experiments were able to grow under environment conditions that were similar to that of the Gale Crater's aqueous environment at Yellowknife Bay. The analysis of simulated Martian water-rock systems after dissolution experiments identified mineralogical, microscopic and geochemical changes characteristic to the biotic test group that could be interpreted as potential bio-signatures. These changes are likely to be caused by the action of anaerobic microbes, analogues to those that could have existed in early Gale Crater aqueous system and would have enhanced mineral weathering and promoted secondary mineral formation. Thermochemical modelling has highlighted more significant differences between fluid chemistries and secondary alteration minerals that would form in reducing biotic and abiotic systems over geological time scales. Under biomediated lacustrine-sedimentary conditions, a 'simpler' mineral assemblage is predicted to precipitate during long-term weathering. Quartz, carbonates and Fe-sulfides are the main secondary minerals to form under biotic conditions, whereas in the abiotic system Fe-oxides and phyllosilicate, in addition to the aforementioned minerals, also precipitate. Since Gale and Jezero Craters are the targets of current and future *in-situ* Mars exploration missions, identification and characterisation of geochemical bio-signatures produced by analogue microbial communities from terrestrial fluvio-lacustrine systems is important to determine the potential habitability of similar environments on early Mars. The results of this study reinforce the necessity to use complex analogue microbial communities and to combine laboratory experiments with thermochemical modelling when investigating the formation of inorganic bio-signatures that form over geological timescales, particularly where those studies may inform the search for habitable environments. The results obtained here, alone, may be not sufficient as unambiguous bio-signatures for life detection on Mars. However, they could be used in conjunction with other geological, geochemical and biological evidence to assess the presence of life in ancient Martian environments. More studies are required in order to build a more comprehensive body of evidence that can be used to identify, unambiguously, inorganic bio-signatures on Mars. Considering the outcomes of this and previous studies (Olsson-Francis et al., 2017), we want to empathise and tress that only using a more holistic approach that combines experimental microbiology, analytical geochemistry and thermochemical modelling, similarly to what was applied in this study, it will be possible to fully understand the evolution of fluid and rock chemistries under biotic conditions and geochemical bio-signatures formation in low-temperature aqueous systems on early Mars. In this context, thermochemical modelling represents an essential tool that allows to investigate reaction pathways and secondary minerals even at low-temperature when slow reaction rates make their study difficult under laboratory conditions.

Future work, employing a manufactured, multi-component simulant with a mineralogical and chemical composition more similar to the Rocknest basalt at Gale Crater (OUCM-1—Ramkissoon et al., 2019) and a microbial community that more likely to represent life on early Mars (as discussed in Macey et al., in review), could increase the fidelity of the type of inorganic bio-signatures (e.g., the secondary mineral assemblage) that a microbial community could develop under simulated Martian conditions. Also, the use a wider range of analytical techniques (e.g., NIR, FTIR, XRD, XPS, Raman Spectroscopy) relevant to either current (NASA's Mars Science Laboratory and Mars Perseverance) and future (ESA's Rosalind Franklin) Mars missions could help to better characterize the chemical, mineralogical and physical changes that occur on the simulant surface after dissolution experiments. This will inform the possible recognition of inorganic bio-signatures during ongoing exploration missions and the analysis of samples recovered by a future sample return mission.

Data availability statement

The original contributions presented in the study are included in the article/Supplementary Material, further inquiries can be directed to the corresponding author.

Author contributions

SC carried out the thermochemical modelling and interpreted the results and led the writing of the manuscript; EW carried out the microbiology experiments and analyses, the FEG-SEM work and the geochemical analyses; NR carried out preliminary thermochemical modelling and took part in manuscript revision; KO-F conceptualized and supervised the study, took part in microbial data analysis and manuscript writing; SS assisted in conceptualizing and supervising the study, took part in the interpretation of the thermochemical model results; VP assisted in supervising the study and took part in manuscript writing.

Funding

This work was supported by Research England Expanding Excellence in England (E3) fund (Grant code 124.18), as well as an STFC funded studentship awarded to EW, and United Kingdom Space Agency grant ST/S001522/1 to SS.

Conflict of interest

The authors declare that the research was conducted in the absence of any commercial or financial relationships that could be construed as a potential conflict of interest.

Publisher's note

All claims expressed in this article are solely those of the authors and do not necessarily represent those of their affiliated organizations, or those of the publisher, the editors and the reviewers. Any product that may be evaluated in this article, or claim that may be made by its manufacturer, is not guaranteed or endorsed by the publisher.

Supplementary material

The Supplementary Material for this article can be found online at: https://www.frontiersin.org/articles/10.3389/fspas.2022.1062007/full#supplementary-material

References

Abramov, O., and Kring, D. A. (2005). Impact-induced hydrothermal activity on early Mars. *J. Geophys. Res.* 110 (E12), S09. doi:10.1029/2005je002453

Akbulut, A., and Kadir, S. (2003). Huntite deposits in the neogene lacustrine sediments of the Cameli basin, Denizli, SW Turkey. *Carbonates Evaporites* 18, 1–9. doi:10.1007/bf03178382

Allwood, B. C., Wade, L. A., Foote, M. C., Elam, W. T., Hurowitz, J. A., Battel, S., et al. (2020). Pixl: Planetary instrument for X-ray Lithochemistry. *Space Sci. Rev.* 216 (8), 134. doi:10.1007/s11214-020-00767-7

Amils, R., González-Toril, E., Fernández-Remolar, D., Gómez, F., Aguilera, Á., Rodríguez, N., et al. (2007). Extreme environments as Mars terrestrial analogs: The Rio Tinto case. *Planet. Space Sci.* 55 (3), 370–381. doi:10.1016/j.pss.2006.02.006

Archer, P. D., Jr., Rampe, E. B., Clark, J. V., Tu, V., Sutter, B., Vaniman, D., et al. (2020). "Detection of siderite ($FeCO_3$) in glen torridon samples by the mars science laboratory rover," in 51st Lunar and Planetary Science Conference (Houston, TX: Lunar and Planetary Institute). abstract 2709.

Arvidson, R. E., Squyres, S. W., Bell, J. F., Catalano, J. G., Clark, B. C., Crumpler, L. S., et al. (2014). Ancient aqueous environments at endeavour crater, mars. *Science* 343 (6169), 1248097. doi:10.1126/science.1248097

Balch, W. E., Fox, G. E., Magrum, L. J., Woese, C. R., and Wolfe, R. S. (1979). Methanogens: Reevaluation of a unique biological group. *Microbiol. Rev.* 43, 260–296. doi:10.1128/mr.43.2.260-296.1979

Banfield, J. F., Moreau, J. W., Chan, C. S., Welch, S. A., and Little, B. (2001). Mineralogical bio-signatures and the search for life on Mars. *Astrobiology* 1 (4), 447–465. doi:10.1089/153110701753593856

Barker, W. W., and Banfield, J. F. (1998). Zones of chemical and physical interaction at interfaces between microbial communities and minerals: A model. *Geomicrobiol. J.* 15 (3), 223–244. doi:10.1080/01490459809378078

Barker, W. W., Welch, S. A., Chu, S., and Banfield, J. F. (1998). Experimental observations of the effects of bacteria on aluminosilicate weathering. *Am. Mineral.* 83, 1551–1563. doi:10.2138/am-1998-11-1243

Bennet, P. C., Rogers, J. R., and Choi, W. J. (2001). Silicates, silicate weathering, and microbial ecology. *Geomicrobiol. J.* 18, 3–19. doi:10.1080/01490450151079734

Benzerara, K., Barakat, M., Menguy, N., Guyot, F., De Luca, G., Audrain, C., et al. (2004). Experimental colonization and alteration of orthopyroxene by the Pleomorphic Bacteria Ramlibacter tataouinensis. *Geomicrobiol. J.* 21 (5), 341–349. doi:10.1080/01490450490462039

Benzerara, K., Menguy, N., Guyot, F., Vanni, C., and Gillet, P. (2005). TEM study of a silicate-carbonate-microbe interface prepared by focused ion beam milling. *Geochimica Cosmochimica Acta* 69 (6), 1413–1422. doi:10.1016/j.gca.2004.09.008

Berg, J. S., Duverger, A., Cordier, L., Laberty-Robert, C., Guyot, F., and Miot, J. (2020). Rapid pyritization in the presence of a sulfur/sulfate-reducing bacterial consortium. *Sci. Rep.* 10 (1), 8264. doi:10.1038/s41598-020-64990-6

Bibring, J. P., Langevin, Y., Mustard, J. F., Poulet, F., Arvidson, R., Gendrin, A., et al. (2005). Global mineralogical and aqueous Mars history derived from OMEGA/Mars Express data. *Science* 312 (5772), 400–404. doi:10.1126/science.1122659

Blake, D. F., Morris, R. V., Kocurek, G., Morrison, S. M., Downs, R. T., Bish, D., et al. (2013). Curiosity at Gale crater, mars: Characterization and analysis of the rocknest sand shadow. *Science* 341, 1239505. doi:10.1126/science.1239505

Boston, P. J., Spilde, M. N., Northup, D. E., Melim, L. A., Soroka, D. S., Kleina, L. G., et al. (2001). Cave bio-signature suites: Microbes, minerals, and mars. *Astrobiology* 1 (1), 25–55. doi:10.1089/153110701750137413

Brantley, S. L., and Chen, Y. (1995). Chemical weathering rates of pyroxenes and amphiboles. *Rev. Miner.* 31, 119–172.

Bricker, O. P., Nesbitt, H. W., and Gunter, W. D. (1973). Stability of talc. *Am. Mineralogist* 58, 64–72.

Bridges, J. C., Hicks, L. J., and Treiman, A. H. (2019). "Carbonates on mars," in *Volatiles in the martian crust*. Editors J. Filiberto and S. P. Schwenzer (Elsevier), 89–118.

Bridges, J. C., Schwenzer, S. P., Leveille, R., Westall, F., Wiens, R. C., Mangold, N., et al. (2015). Diagenesis and clay mineral formation at Gale crater, mars. *J. Geophys. Res. Planets* 120, 1–19. doi:10.1002/2014je004757

Bridges, J. C., and Schwenzer, S. P. (2012). The nakhlite hydrothermal brine on Mars. *Earth Planet. Sci. Lett.* 359-360, 117–123. doi:10.1016/j.epsl.2012.09.044

Bristow, T. F., Grotzinger, J. P., Rampe, E. B., Cuadros, J., Chipera, S. J., Downs, G. W., et al. (2021). Brine-driven destruction of clay minerals in Gale crater, mars. *Science* 373 (6551), 198–204. doi:10.1126/science.abg5449

Bultel, B., Viennet, J. C., Poulet, F., Carter, J., and Werner, S. C. (2019). Detection of carbonates in Martian weathering profiles. *J. Geophys. Res. Planets* 124, 989–1007. doi:10.1029/2018je005845

Cady, S. L., Farmer, J. D., Grotzinger, J. P., Schopf, J. W., and Steele, A. (2003). Morphological bio-signatures and the search for life on Mars. *Astrobiology* 3 (2), 351–368. doi:10.1089/153110703769016442

Carr, M. H., and Head, J. W. (2010). Geologic history of mars. *Earth Planet. Sci. Lett.* 294 (3–4), 185–203. doi:10.1016/j.epsl.2009.06.042

Carter, D. L., Mangold, N., Poulet, F., and Bibring, J. P. (2015). Widespread surface weathering on early mars: A case for a warmer and wetter climate. *Icarus* 248, 373–382. doi:10.1016/j.icarus.2014.11.011

Carter, J., Poulet, F., Bibring, J. P., Mangold, N., and Murchie, S. (2013). Hydrous minerals on Mars as seen by the CRISM and OMEGA imaging spectrometers: Updated global view. *J. Geophys. Res. Planets* 118 (4), 831–858. doi:10.1029/2012je004145

Catalano, J. G. (2013). Thermodynamic and mass balance constraints on iron-bearing phyllosilicate formation and alteration pathways on early Mars. *J. Geophys. Res. Planets* 118, 2124–2136. doi:10.1002/jgre.20161

Changela, H. G., and Bridges, J. C. (2011). Alteration assemblages in the nakhlites: Variation with depth on Mars. *Meteorit. Planet. Sci.* 45, 1847–1867. doi:10.1111/j.1945-5100.2010.01123.x

Christensen, P. R., McSween, H. Y., Bandfield, J. L., Ruff, S. W., Rogers, A. D., Hamilton, V. E., et al. (2005). Evidence for magmatic evolution and diversity on Mars from infrared observations. *Nature* 436, 504–509. doi:10.1038/nature03639

Cockell, C. S., Bush, T., Bryce, C., Direito, S., Fox-Powell, M., Harrison, J. P., et al. (2016). Habitability: A review. *Astrobiology* 16 (1), 89–117. doi:10.1089/ast.2015.1295

Cole, W. F., and Lancucki, C. J. (1975). Huntite from deer park, victoria, Australia. *Am. Mineralogist* 60, 1130–1131.

Conrad, P. G. (2014). Scratching the surface of martian habitability. *Science* 346 (6215), 1288–1289. doi:10.1126/science.1259943

Curtis-Harper, E., Pearson, V. K., Summers, S., Bridges, J. C., Schwenzer, S. P., and Olsson-Francis, K. (2018). The microbial community of a terrestrial anoxic inter-tidal zone: A model for laboratory-based studies of potentially habitable ancient lacustrine systems on mars. *Microorganisms* 6 (3), 61. doi:10.3390/microorganisms6030061

Dartnell, L. R. (2011). Ionizing radiation and life. *Astrobiology* 11, 551–582. doi:10.1089/ast.2010.0528

Duverger, A., Berg, J. S., Busigny, V., Guyot, F., Bernard, S., and Miot, J. (2020). Mechanisms of pyrite formation promoted by sulfate-reducing bacteria in pure culture. *Front. Earth Sci. (Lausanne).* 8, 588310. doi:10.3389/feart.2020.588310

Edgar, L. A., Fedo, C. M., Gupta, S., Banham, S. G., Fraeman, A. A., Grotzinger, J. P., et al. (2020). A lacustrine paleoenvironment recorded at vera rubin ridge, Gale crater: Overview of the sedimentology and stratigraphy observed by the mars science laboratory curiosity rover. *JGR. Planets* 125, e2019JE006307. doi:10.1029/2019je006307

Edgett, K. S., Yingst, R. A., Ravine, M. A., Caplinger, M. A., Maki, J. N., Ghaemi, F. T., et al. (2012). Curiosity's mars Hand Lens imager (MAHLI) investigation. *Space Sci. Rev.* 170 (1–4), 259–317. doi:10.1007/s11214-012-9910-4

Ehlmann, B. L., Berger, G., Mangold, N., Michalski, J. R., Catling, D. C., Ruff, S. W., et al. (2013). Geochemical consequences of widespread clay mineral formation in Mars' ancient crust. *Space Sci. Rev.* 174, 329–364. doi:10.1007/s11214-012-9930-0

Ehlmann, B. L., and Edwards, C. S. (2014). Mineralogy of the martian surface. *Annu. Rev. Earth Planet. Sci.* 42 (1), 291–315. doi:10.1146/annurev-earth-060313-055024

Ehlmann, B. L., Mustard, J. F., Murchie, S. L., Poulet, F., Bishop, J. L., Brown, A. J., et al. (2008). Orbital identification of carbonate-bearing rocks on Mars. *Science* 322 (5909), 1828–1832. doi:10.1126/science.1164759

Ehlmann, B. L., Mustard, J. F., Swayze, G. A., Clark, R. N., Bishop, J. L., Poulet, F., et al. (2009). Identification of hydrated silicate minerals on Mars using MRO-CRISM: Geologic context near Nili Fossae and implications for aqueous alteration. *J. Geophys. Res.* 114, E00D08. doi:10.1029/2009je003339

Ehlmann, B., Mustard, J., Murchie, S., Bibring, J-P., Meunier, A., Fraeman, A. A., et al. (2011). Subsurface water and clay mineral formation during the early history of Mars. *Nature* 479, 53–60. doi:10.1038/nature10582

Ehrenfried, M. (2022). *Perseverance and the Mars 2020 mission: Follow the science to Jezero Crater*, XVIII. Springer Cham, 258.

Ehrlich, H. L., and Newman, D. K. (2009). *Geomicrobiology*. 5th ed. Boca Raton: Taylor & Francis, 628.

Fassett, C. I., and Head, J. W. (2015). Fluvial sedimentary deposits on mars: Ancient deltas in a crater lake in the Nili Fossae region. *Geophys. Res. Lett.* 32. doi:10.1029/2005gl023456

Filiberto, J., and Schwenzer, S. P. (2013). Alteration mineralogy of Home Plate and Columbia Hills Formation conditions in context to impact, volcanism, and fluvial activity. *Meteorit. Planet. Sci.* 48, 1937–1957. doi:10.1111/maps.12207

Filiberto, J. (2008). Similarities between the shergottites and terrestrial ferropicrites. *Icarus* 197, 52–59. doi:10.1016/j.icarus.2008.04.016

Fox, V. K., Arvidson, R. E., Guinness, E. A., McLennan, S. M., Catalano, J. G., Murchie, S. L., et al. (2016). Smectite deposits in Marathon Valley, Endeavour Crater, Mars, identified using CRISM hyperspectral reflectance data. *Geophys. Res. Lett.* 43, 4885–4892. doi:10.1002/2016gl069108

Fraeman, A. A., Edgar, L. A., Rampe, E. B., Thompson, L. M., Frydenvang, J., Fedo, C. M., et al. (2020). Evidence for a diagenetic origin of vera rubin ridge, Gale crater, mars: Summary and synthesis of Curiosity's exploration campaign. *J. Geophys. Res. Planets* 125, e2020JE006527. doi:10.1029/2020je006527

Gadd, G. M. (2010). Metals, minerals and microbes: Geomicrobiology and bioremediation. *Microbiology* 156 (3), 609–643. doi:10.1099/mic.0.037143-0

Garrels, R. M., Thompson, M. E., and Siever, R. (1960). Stability of some carbonates at 25 ^{O}C and one atmosphere total pressure. *Am. J. Sci.* 258, 402–418. doi:10.2475/ajs.258.6.402

Gislason, S. R., and Eugster, H. P. (1987). Meteoric water-basalt interactions. I: A laboratory study. *Geochimica Cosmochimica Acta* 51, 2827–2840. doi:10.1016/0016-7037(87)90161-x

Goudge, T. A., Mustard, J. F., Head, J. W., Fassett, C. I., and Wiseman, S. M. (2015). Assessing the mineralogy of the watershed and fan deposits of the Jezero Crater paleolake system, Mars. *J. Geophys. Res. Planets* 120, 775–808. doi:10.1002/2014je004782

Griffith, L. L., and Shock, E. L. (1997). Hydrothermal hydration of Martian crust: Illustration via geochemical model calculations. *J. Geophys. Res.* 102 (E4), 9135–9143. doi:10.1029/96je02939

Grigsby, J. D. (2001). Origin and growth mechanism of authigenic chlorite in sandstones of the Lower Vicksburg Formation, South Texas. *J. Sediment. Res.* 71, 27–36. doi:10.1306/060100710027

Grotzinger, J. P., Crisp, J., Vasavada, A. R., Anderson, R. C., Baker, C. J., Barry, R., et al. (2012). Mars science laboratory mission and science investigation. *Space Sci. Rev.* 170, 5–56. doi:10.1007/s11214-012-9892-2

Grotzinger, J. P., Gupta, S., Malin, M. C., Rubin, D. M., Schieber, J., Siebach, K., et al. (2015). Deposition, exhumation, and paleoclimate of an ancient lake deposit, Gale Crater, Mars. *Science* 350, aac7575. doi:10.1126/science.aac7575

Grotzinger, J. P., Sumner, D. Y., Kah, L. C., Stack, K., Gupta, S., Edgar, L., et al. (2014). Deposition, exhumation, and paleoclimate of an ancient lake deposit, Gale crater, Mars. *Science* 343 (6169), aac7575. doi:10.1126/science.aac7575

Hand, K. P., Carlson, R. W., and Chyba, C. F. (2007). Energy, chemical disequilibrium and geological constraints on Europa. *Astrobiology* 7, 1006–1022. doi:10.1089/ast.2007.0156

Hays, L. E., Graham, H. V., Des Marais, D. J., Hausrath, E. M., Horgan, B., McCollom, T. M., et al. (2017). Bio-signature preservation and detection in mars analog environments. *Astrobiology* 17 (4), 363–400. doi:10.1089/ast.2016.1627

Hiebert, F. K., and Bennett, P. C. (1992). Microbial control of silicate weathering in organic-rich ground water. *Science* 258 (5080), 278–281. doi:10.1126/science.258.5080.278

Horgan, B. H. N., Anderson, R. B., Dromart, G., Amador, E. S., and Rice, M. S. (2020). The mineral diversity of Jezero Crater: Evidence for possible lacustrine carbonates on Mars. *Icarus* 339, 113526. doi:10.1016/j.icarus.2019.113526

Hungate, R. E. (1966). *The rumen and its Microbes*. Academic Press, 1–533.

Hurowitz, J. A., Grotzinger, J. P., Fischer, W. W., McLennan, S. M., Milliken, R. E., Stein, N., et al. (2017). Redox stratification of an ancient lake in Gale crater, mars. *Science* 356, 6849. doi:10.1126/science.aah6849

Huston, D. L., and Logan, G. A. (2004). Barite, BIFs and bugs: Evidence for the evolution of the Earth's early hydrosphere. *Earth Planet. Sci. Lett.* 220, 41–55. doi:10.1016/s0012-821x(04)00034-2

Irwin, R. P., Howard, A. D., Craddock, R. A., and Moore, J. M. (2005). An intense terminal epoch of widespread fluvial activity on early mars: 2. Increased runoff and paleolake development. *J. Geophys. Res.* 110, S15–S38. doi:10.1029/2005je002460

Kalinowski, B. E., Liermann, L. J., Givens, S., and Brantley, S. L. (2000). Rates of bacteria-promoted solubilization of Fe from minerals: A review of problems and approaches. *Chem. Geol.* 169 (3-4), 357–370. doi:10.1016/s0009-2541(00)00214-x

Kinsman, D. J. J. (1967). Huntite from a carbonate-evaporite environment. *Am. Mineralogist* 52, 1332.

Konhauser, K. (2007). *Introduction to geomicrobiology*. Wiley-Blackwell, 440.

Kühn, M. (2004). "Reactive flow modeling of hydrothermal systems," in *Lecture notes in earth Sciences* (Berlin: Springer).

Lee, M. K., Griffin, J., Saunders, J., Wang, Y., and Jean, J. S. (2007). Reactive transport of trace elements and isotopes in the Eutaw coastal plain aquifer, Alabama. *J. Geophys. Res.* 112, G02026. doi:10.1029/2006jg000238

Lian, B., Chen, Y., Zhu, L., and Yang, R. (2008). Effect of microbial weathering on carbonate rocks. *Earth Sci. Front.* 15 (6), 90–99. doi:10.1016/s1872-5791(09)60009-9

Liermann, L. J., Barnes, A. S., Kalinowski, B. E., Zhou, X., and Brantley, S. L. (2000). Microenvironments of pH in biofilms grown on dissolving silicate surfaces. *Chem. Geol.* 171 (1–2), 1–16. doi:10.1016/s0009-2541(00)00202-3

Longhi, J., Knittle, E., Holloway, J., and Waenke, H. (1992). The bulk composition, mineralogy and internal structure of Mars. *Mars* 1, 184–208. doi:10.2307/j.ctt207g59v.10

Lüttge, A., and Conrad, P. G. (2004). Direct observation of microbial inhibition of calcite dissolution. *Appl. Environ. Microbiol.* 70 (3), 1627–1632. doi:10.1128/aem.70.3.1627-1632.2004

Malin, M., and Edgett, K. (2003). Evidence for persistent flow and aqueous sedimentation on early mars. *Science* 302, 1931–1934. doi:10.1126/science.1090544

Mangold, N., Adeli, S., Conway, S., Ansan, V., and Langlais, B. (2012). A chronology of early Mars climatic evolution from impact Crater degradation. *J. Geophys. Res.* 117. doi:10.1029/2011je004005

Mangold, N., Gupta, S., Gasnault, O., Dromart, G., Tarnas, J. D., Sholes, S. F., et al. (2021). Perseverance rover reveals an ancient delta-lake system and flood deposits at Jezero Crater, Mars. *Science* 374 (6568), 711–717. doi:10.1126/science.abl4051

Mangold, N., Schmidt, M. E., Fisk, M. R., Forni, O., McLennan, S. M., Ming, D. W., et al. (2017). Classification scheme for sedimentary and igneous rocks in Gale Crater, Mars. *Icarus* 284, 1–17. doi:10.1016/j.icarus.2016.11.005

Marini, L. (2007). "Geological sequestration of carbon dioxide: Thermodynamics, kinetics, and reaction path modeling," in *Developments in geochemistry* (New York, New York: Elsevier), 11.

Marion, G. M., Kargel, J. S., and Catling, D. C. (2008). Modeling ferrous–ferric iron chemistry with application to martian surface geochemistry. *Geochimica Cosmochimica Acta* 72 (1), 242–266. doi:10.1016/j.gca.2007.10.012

Marzo, G. A., Davila, A. F., Tornabene, L. L., Dohm, J. M., Fairén, A. G., Gross, C., et al. (2010). Evidence for hesperian impact-induced hydrothermalism on mars. *Icarus* 208 (2), 667–683. doi:10.1016/j.icarus.2010.03.013

McMahon, S., Bosak, T., Grotzinger, J. P., Milliken, R. E., Summons, R. E., Daye, M., et al. (2018). A field guide to finding fossils on Mars. *JGR. Planets* 123, 1012–1040. doi:10.1029/2017je005478

Melwani Daswani, M., Schwenzer, S. P., Reed, M. H., Wright, I. P., and Grady, M. M. (2016). Alteration minerals, fluids, and gases on early Mars: Predictions from 1-D flow geochemical modeling of mineral assemblages in meteorite ALH 84001. *Meteorit. Planet. Sci.* 51, 2154–2174. doi:10.1111/maps.12713

Minitti, M. E., Kah, L. C., Yingst, R. A., Edgett, K. S., Anderson, R. C., Beegle, L. W., et al. (2013). MAHLI at the Rocknest sand shadow: Science and science-enabling activities. *J. Geophys. Res. Planets* 118, 2338–2360. doi:10.1002/2013je004426

Molina-Cuberos, G. J., Stumptner, W., Lammer, H., and Komle, N. I. (2001). Cosmic ray and UV radiation models on the ancient martian surface. *Icarus* 154, 216–222. doi:10.1006/icar.2001.6658

Morris, R. V., Vaniman, D. T., Blake, D. F., Gellert, R., Chipera, S. J., Rampe, E. B., et al. (2016). Silicic volcanism on Mars evidenced by tridymite in high-SiO_2 sedimentary rock at Gale Crater. *Proc. Natl. Acad. Sci. U. S. A.* 113, 7071–7076. doi:10.1073/pnas.1607098113

Mustard, J. F., Murchie, S. L., Pelkey, S. M., Ehlmann, B. L., Milliken, R. E., Grant, J., et al. (2008). Hydrated silicate minerals on mars observed by the mars reconnaissance orbiter CRISM instrument. *Nature* 454 (7202), 305–309. doi:10.1038/nature07097

Nahon, D. B., and Colin, F. (1982). Chemical weathering of orthopyroxenes under lateritic conditions. *Am. J. Sci.* 282 (8), 1232–1243. doi:10.2475/ajs.282.8.1232

Niles, P. B., Catling, D. C., Berger, G., Chassefière, E., Ehlmann, B. L., Michalski, J. R., et al. (2013). Geochemistry of carbonates on mars: Implications for climate history and nature of aqueous environments. *Space Sci. Rev.* 174 (1-4), 301–328. doi:10.1007/s11214-012-9940-y

Nixon, S. L., Cousins, C. R., and Cockell, C. S. (2013). Plausible microbial metabolisms on Mars. *Astronomy Geophys.* 54 (1), 1.13–1.16. doi:10.1093/astrogeo/ats034

Nyquist, L. E., Bogard, D. D., Shih, C. Y., Greshake, A., Stoffler, D., and Eugster, O. (2001). Ages and geologic histories of martian meteorites. *Space Sci. Rev.* 96, 105–164. doi:10.1023/a:1011993105172

Oelkers, E. H., and Gislason, S. R. (2001). The mechanism, rates and consequences of basaltic glass dissolution: I. An experimental study of the dissolution rates of basaltic glass as a function of aqueous Al, Si and oxalic acid concentration at 25°C and pH=3 and 11. *Geochimica Cosmochimica Acta* 65 (21), 3671–3681. doi:10.1016/s0016-7037(01)00664-0

Olsson-Francis, K., Boardman, C. P., Pearson, V. K., Schofield, P. F., Oliver, A., and Summers, S. (2015). A culture-independent and culture-dependent study of the bacterial community from the bedrock soil interface. *Adv. Microbiol.* 5, 842–857. doi:10.4236/aim.2015.513089

Olsson-Francis, K., De La Torre, R., and Cockell, C. S. (2010). Isolation of novel extreme-tolerant cyanobacteria from a rock-dwelling microbial community by using exposure to low Earth orbit. *Appl. Environ. Microbiol.* 76 (7), 2115–2121. doi:10.1128/aem.02547-09

Olsson-Francis, K., Pearson, V. K., Schofield, P. F., Oliver, A., and Summers, S. (2016). A study of the microbial community at the interface between granite bedrock and soil using a culture-independent and culture-dependent approach. *Adv. Microbiol.* 6 (3), 233–245. doi:10.4236/aim.2016.63023

Olsson-Francis, K., Pearson, V. K., Steer, E. D., and Schwenzer, S. P. (2017). Determination of geochemical bio-signatures in Mars-like basaltic environments. *Front. Microbiol.* 8, 1668. doi:10.3389/fmicb.2017.01668

Olsson-Francis, K., Ramkissoon, N. K., Macey, M., Pearson, V. K., Schwenzer, S. P., and Johnson, D. N. (2020). Simulating microbial processes in extraterrestrial, aqueous environments. *J. Microbiol. Methods* 172, 105883. doi:10.1016/j.mimet.2020.105883

Olsson-Francis, K., Simpson, E., Wolff-Boenisch, D., and Cockell, C. S. (2012). The effect of rock composition on cyanobacterial weathering of crystalline basalt and rhyolite. *Geobiology* 10 (5), 434–444. doi:10.1111/j.1472-4669.2012.00333.x

Osinski, G. R., Tornabene, L. L., Banerjee, N. R., Cockell, C. S., Flemming, R., Izawa, M. R. M., et al. (2013). Impact-generated hydrothermal systems on earth and mars. *Icarus* 224 (2), 347–363. doi:10.1016/j.icarus.2012.08.030

Palandri, J. L., and Reed, M. H. (2004). Geochemical models of metasomatism in ultramafic systems: Serpentinization, rodingitization, and sea floor carbonate chimney precipitation. *Geochimica Cosmochimica Acta* 68, 1115–1133. doi:10.1016/j.gca.2003.08.006

Palomba, E., Zinzi, A., Cloutis, E. A., D'Amore, M., Grassi, D., and Maturilli, D. (2009). Evidence for Mg-rich carbonates on Mars from a 3.9 μm absorption feature. *Icarus* 203 (1), 58–65. doi:10.1016/j.icarus.2009.04.013

Poulet, F., Bibring, J. P., Mustard, J. F., Gendrin, A., Mangold, N., Langevin, Y., et al. (2005). Phyllo-silicates on Mars and implications for early Martian climate. *Nature* 438, 623–627. doi:10.1038/nature04274

Poulet, F., Gomez, C., Bibring, J. P., Langevin, Y., Gondet, B., Pinet, P., et al. (2007). Martian surface mineralogy from Observatoire pour la Minéralogie, l'Eau, les Glaces et l'Activité on board the Mars Express spacecraft (OMEGA/MEX): Global mineral maps. *J. Geophys. Res.* 112, E08S02. doi:10.1029/2006je002840

Price, A., Pearson, V. K., Schwenzer, S. P., Miot, J., and Olsson-Francis, K. (2018). Nitrate-dependent iron oxidation: A potential Mars metabolism. *Front. Microbiol.* 9, 513. doi:10.3389/fmicb.2018.00513

Ramkissoon, N. K., Pearson, V. K., Schwenzer, S. P., Schröder, C., Kirnbauer, T., Wood, D., et al. (2019). New simulants for martian regolith: Controlling iron variability. *Planet. Space Sci.* 179, 104722. doi:10.1016/j.pss.2019.104722

Ramkissoon, N. K., Turner, S. M. R., Macey, M. C., Schwenzer, S. P., Reed, M. H., Pearson, V. K., et al. (2021). Exploring the environments of Martian impact-generated hydrothermal systems and their potential to support life. *Meteorit. Planet. Sci.* 56, 1350–1368. doi:10.1111/maps.13697

Rampe, E. B., Blake, D. F., Bristow, T. F., Ming, D. W., Vaniman, D. T., Morris, R. V., et al. (2020). Mineralogy and geochemistry of sedimentary rocks and eolian sediments in Gale crater, mars: A review after six earth years of exploration with curiosity. *Geochemistry* 80 (2), 125605. doi:10.1016/j.chemer.2020.125605

Rampe, E. B., Ming, D. W., Blake, D. F., Bristow, T. F., Chipera, S. J., Grotzinger, J. P., et al. (2017). Mineralogy of an ancient lacustrine mudstone succession from the Murray formation, Gale Crater, Mars. *Earth Planet. Sci. Lett.* 471, 172–185. doi:10.1016/j.epsl.2017.04.021

Rapin, W., Dromart, G., Rubin, D., Le Deit, L., Mangold, N., Edgar, L. A., et al. (2021). Alternating wet and dry depositional environments recorded in the stratigraphy of Mount Sharp at Gale Crater. Mars. *Geology* 49 (7), 842–846. doi:10.1130/g48519.1

Reed, M. H. (1982). Calculation of multicomponent chemical equilibria and reaction processes in systems involving minerals, gases and an aqueous phase. *Geochimica Cosmochimica Acta* 46, 513–528. doi:10.1016/0016-7037(82)90155-7

Reed, M. H., Spycher, N. F., and Palandri, J. (2010). *Users guide for CHIM-XPT: A program for computing reaction processes in aqueous-mineral-gas systems and MINTAB guide*. Eugene, OR: University of Oregon.

Reed, M. H., and Spycher, N. F. (2006). *User guide for CHILLER: A program for computing water-rock reactions, boiling, mixing and other reaction processes in aqueous-mineral-gas systems and minplot guide*. Eugene, OR: University of Oregon.

Rogers, J. R., Bennett, P. C., and Choi, W. J. (1998). Feldspars as a source of nutrients for microorganisms. *Am. Mineralogist* 83 (11-12), 1532–1540. doi:10.2138/am-1998-11-1241

Röling, W. F. M., Aerts, J. W., Patty, C. H. L., Ten Kate, I. L., Ehrenfreund, P., and Direito, S. O. L. (2015). The significance of microbe-mineral-biomarker interactions in the detection of life on mars and beyond. *Astrobiology* 15 (6), 492–507. doi:10.1089/ast.2014.1276

Schmidt, M. E., Campbell, J. L., Gellert, R., Perrett, G. M., Treiman, A. H., Blaney, D. L., et al. (2014). Geochemical diversity in first rocks examined by the Curiosity rover in Gale Crater: Evidence for and significance of an alkali and volatile-rich igneous source. *J. Geophys. Res. Planets* 119 (1), 64–81. doi:10.1002/2013je004481

Schulte, M., Blake, D., Hoehler, T., and McCollom, T. (2006). Serpentinization and its implications for life on the early earth and mars. *Astrobiology* 6, 364–376. doi:10.1089/ast.2006.6.364

Schwenzer, S. P., Abramov, O., Allen, C. C., Bridges, J. C., Clifford, S. M., Filiberto, J., et al. (2012). Gale Crater: Formation and post-impact hydrous environments. *Planet. Space Sci.* 70 (1), 84–95. doi:10.1016/j.pss.2012.05.014

Schwenzer, S. P., and Kring, D. A. (2013). Alteration minerals in impact-generated hydrothermal systems - exploring host rock variability. *Icarus* 226, 487–496. doi:10.1016/j.icarus.2013.06.003

Schwenzer, S. P., and Kring, D. A. (2009). Impact-generated hydrothermal systems capable of forming phyllosilicates on Noachian Mars. *Geology* 37, 1091–1094. doi:10.1130/g30340a.1

Speers, A. M., Cologgi, D. L., and andReguera, G. (2009). Anaerobic cell culture. *Curr. Protoc. Microbiol.* 12, A.4F.1–A.4F.16. doi:10.1002/9780471729259.mca04fs12

Spotl, C., and Burns, S. J. (1994). Magnesite diagenesis in redbeds: A case study from the permian of the northern calcareous alps (tyrol, Austria). *Sedimentology* 41, 543–565. doi:10.1111/j.1365-3091.1994.tb02010.x

Stanger, G., and Neal, C. (1994). The occurrence and chemistry of huntite from Oman. *Chem. Geol.* 112, 247–254. doi:10.1016/0009-2541(94)90027-2

Stern, J. C., Sutter, B., Navarro-gonzález, R., Mckay, C. P., Jr, P. D. A., Buch, A., et al. (2015). Freissinet, C. and the MSL Science Team-20Evidence for indigenous nitrogen in sedimentary and aeolian deposits from the Curiosity rover investigations at Gale Crater, Mars. *Proc. Natl. Acad. Sci. U. S. A.* 112 (23), 4245–4250. doi:10.1073/pnas.1420932112

Summons, R. E., Amend, J. P., Bish, D., Buick, R., Cody, G. D., Des Marais, D. J., et al. (2011). Preservation of martian organic and environmental records: Final report of the mars bio-signature working group. *Astrobiology* 11 (2), 157–181. doi:10.1089/ast.2010.0506

Sun, S., Chan, L. S., and Li, Y.-L. (2014). Flower-like apatite recording microbial processes through deep geological time and its implication to the search for mineral records of life on Mars. *Am. Mineralogist* 99 (10), 2116–2125. doi:10.2138/am-2014-4794

Tan, J., Lewis, J. M. T., and Sephton, M. A. (2018). The fate of lipid bio-signatures in a Mars-analogue sulfur stream. *Sci. Rep.* 8, 7586–7588. doi:10.1038/s41598-018-25752-7

Ten Kate, I. L., Garry, J. R., Peeters, Z., Quinn, R., Foing, B., and Ehrenfreund, P. (2005). Amino acid photostability on the Martian surface. *Meteorit. Planet. Sci.* 40 (8), 1185–1193. doi:10.1111/j.1945-5100.2005.tb00183.x

Thorpe, M. T., Bristow, T. F., Rampe, E. B., Grotzinger, J. P., Fox, V. K., Bennett, K. A., et al. (2020). "Glen Torridon mineralogy and the sedimentary history of the clay mineral bearing unit [abstract 1524]," in 51st Lunar and Planetary Science Conference (Houston, TX: Lunar and Planetary Institute).

Thorseth, I. H., Furnes, H., and Heldal, M. (1992). The importance of microbiological activity in the alteration of natural basaltic glass. *Geochimica Cosmochimica Acta* 56, 845–850. doi:10.1016/0016-7037(92)90104-q

Tian, F., Kasting, J. F., and Solomon, S. C. (2009). Thermal escape of carbon from the early Martian atmosphere. *Geophys. Res. Lett.* 36. doi:10.1029/2008gl036513

Tosca, N. J., Macdonald, F. A., Strauss, J. V., Johnston, D. T., and Knoll, A. H. (2011). Sedimentary talc in Neoproterozoic carbonate successions. *Earth Planet. Sci. Lett.* 306 (1-2), 11–22. doi:10.1016/j.epsl.2011.03.041

Treiman, A. H., and Filiberto, J. (2015). Geochemical diversity of shergottite basalts: Mixing and fractionation, and their relation to mars surface basalts. *Meteorit. Planet. Sci.* 50, 632–648. doi:10.1111/maps.12363

Tu, V. M., Rampe, E. B., Bristow, T. F., Thorpe, M. T., Clark, J. V., Castle, N., et al. (2021). A review of the phyllosilicates in Gale crater as detected by the CheMin instrument on the mars science laboratory, curiosity rover. *Miner. (Basel).* 11 (8), 847. doi:10.3390/min11080847

Turner, S. M. R., Bridges, J. C., Grebby, S., and Ehlmann, B. L. (2016). Hydrothermal activity recorded in post Noachian-aged impact Craters on Mars. *J. Geophys. Res. Planets* 121, 608–625. doi:10.1002/2015je004989

Uroz, S., Calvaruso, C., Turpault, M., Sarniguet, A., de Boer, W., Leveau, J., et al. (2009). Efficient mineral weathering is a distinctive functional trait of the bacterial genus Collimonas. *Soil Biol. Biochem.* 41 (10), 2178–2186. doi:10.1016/j.soilbio.2009.07.031

Vago, J. L., Westall, F., Pasteur Instrument Teams, Landing SCoates, A. J., Jaumann, R., Korablev, O., et al. (2017). Habitability on early mars and the search for biosignatures with the ExoMars rover. *Astrobiology* 17, 471–510. doi:10.1089/ast.2016.1533

Vandevivere, P., Welch, S. A., Ullman, W. J. J., and Kirchman, D. L. L. (1994). Enhanced dissolution of silicate minerals by bacteria at near-neutral pH. *Microb. Ecol.* 27 (3), 241–251. doi:10.1007/bf00182408

Vaniman, D. T., Bish, D. L., Ming, D. W., Bristow, T. F., Morris, R. V., Blake, D. F., et al. (2014). Mineralogy of a mudstone at Yellowknife bay, Gale crater, mars. *Science* 343 (6169), 1243480. doi:10.1126/science.1243480

Weitz, C. M., Sullivan, R. J., Lapotre, M. G. A., Rowland, S. K., Grant, J. A., Baker, M., et al. (2018). Sand grain sizes and shapes in eolian bedforms at Gale Crater, mars. *Geophys. Res. Lett.* 45, 9471–9479. doi:10.1029/2018gl078972

Welch, S. A., Barker, W. W., and Banfield, J. F. (1999). Microbial extracellular polysaccharides and plagioclase dissolution. *Geochim. Cosmochim. Acta* 63 (9), 1405–1419. doi:10.1016/s0016-7037(99)00031-9

Welch, S. A., Taunton, A. E., and Banfield, J. F. (2002). Effect of microorganisms and microbial metabolites on apatite dissolution. *Geomicrobiol. J.* 19 (3), 343–367. doi:10.1080/01490450290098414

Welch, S. A., and Ullman, W. J. (1993). The effect of organic acids on plagioclase dissolution rates and stoichiometry. *Geochimica Cosmochimica Acta* 57, 2725–2736. doi:10.1016/0016-7037(93)90386-b

Welch, S. A., and Vandevivere, P. (1994). Effect of microbial and other naturally occurring polymers on mineral dissolution. *Geomicrobiol. J.* 12 (4), 227–238. doi:10.1080/01490459409377991

Westall, F., Foucher, F., Bost, N., Bertrand, M., Loizeau, D., Vago, J. L., et al. (2015). Bio-signatures on mars: What, where, and how? Implications for the search for martian life. *Astrobiology* 15 (11), 998–1029. doi:10.1089/ast.2015.1374

Widdel, F., Kohring, G. W., and Mayer, F. (1983). Studies on dissimilatory sulfate-reducing bacteria that decompose fatty-acids III. Characterization of the Filamentous Gliding *Desulfonema limicola* gen. nov sp. nov., and *Desulfonema magnum* sp. *Arch. Microbiol.* 134 (4), 286–294. doi:10.1007/bf00407804

Williams, E. R. M., Grotzinger, P. J., Dietrich, E. W., Gupta, S., Sumner, Y. D., Wiens, C. R., et al. (2013). Martian fluvial conglomerates at Gale crater. *Science* 340 (6136), 1068–1072. doi:10.1126/science.1237317

Williford, K. H., Farley, K. A., Stack, K. M., Allwood, A. C., Beaty, D., Beegle, L. W., et al. (2008). "Chapter 11 - the NASA mars 2020 rover mission and the search for extraterrestrial life," in *From habitability to life on Mars*. Editors N. A. Cabrol and E. A. Grin (Elsevier), 275–308.

Wolff-Boenisch, D., Gislason, S. R., and Oelkers, E. H. (2006). The effect of crystallinity on dissolution rates and CO2 consumption capacity of silicates. *Geochimica Cosmochimica Acta* 70, 858–870. doi:10.1016/j.gca.2005.10.016

Wu, L., Jacobson, A. D., Chen, H. C., and Hausner, M. (2007). Characterization of elemental release during microbe–basalt interactions at T=28°C. *Geochimica Cosmochimica Acta* 71 (9), 2224–2239. doi:10.1016/j.gca.2007.02.017

Zolotov, M. Y., and Mironenko, M. V. (2016). Chemical models for martian weathering profiles: Insights into formation of layered phyllosilicate and sulfate deposits. *Icarus* 275, 203–220. doi:10.1016/j.icarus.2016.04.011

Zolotov, M. Y., and Mironenko, M. V. (2007). Timing of acid weathering on mars: A kinetic-thermodynamic assessment. *J. Geophys. Res.* 112, E07006. doi:10.1029/2006je002882